AD-A239 244

MENTATION PAGE

Form Approved
OMB No 0704-0188

1. AGENCY USE ONLY (Leave blank)	2. REPORT DATE	3. REPORT TYPE AND DATES COVERED
		THESIS/~~DISSERTATION~~

4. TITLE AND SUBTITLE
Sediment Transport in Shallow Flow on an Impervious Surface

5. FUNDING NUMBERS

6. AUTHOR(S)
Marvin W. Smith, Jr., Captain

7. PERFORMING ORGANIZATION NAME(S) AND ADDRESS(ES)
AFIT Student Attending: University of Virginia

8. PERFORMING ORGANIZATION REPORT NUMBER
AFIT/CI/CIA- 91-010

9. SPONSORING/MONITORING AGENCY NAME(S) AND ADDRESS(ES)
AFIT/CI
Wright-Patterson AFB OH 45433-6583

10. SPONSORING/MONITORING AGENCY REPORT NUMBER

11. SUPPLEMENTARY NOTES

12a. DISTRIBUTION/AVAILABILITY STATEMENT
Approved for Public Release IAW 190-1
Distributed Unlimited
ERNEST A. HAYGOOD, 1st Lt, USAF
Executive Officer

12b. DISTRIBUTION CODE

13. ABSTRACT *(Maximum 200 words)*

14. SUBJECT TERMS	15. NUMBER OF PAGES 112
	16. PRICE CODE

17. SECURITY CLASSIFICATION OF REPORT	18. SECURITY CLASSIFICATION OF THIS PAGE	19. SECURITY CLASSIFICATION OF ABSTRACT	20. LIMITATION OF ABSTRACT

SEDIMENT TRANSPORT IN SHALLOW FLOW ON AN IMPERVIOUS SURFACE

A thesis

presented to

the faculty of the School of Engineering and Applied Science

University of Virginia

In partial fulfillment

of the requirements for the degree of

Master of Science (Civil Engineering)

by

Marvin W. Smith, Jr.

January 1991

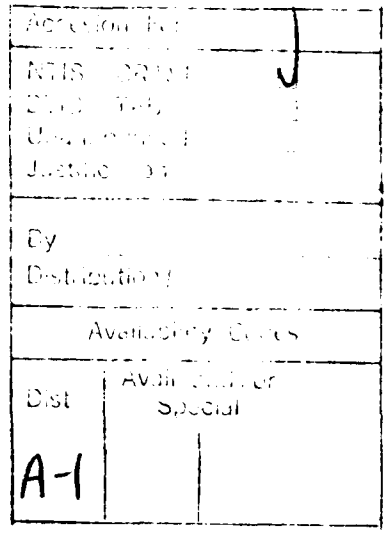

APPROVAL SHEET

This thesis is submitted in partial fulfillment of the requirements for the degree of

Master of Science (Civil Engineering)

AUTHOR

This thesis has been read and approved by the examining Committee:

Thesis advisor

Accepted for the School of Engineering and Applied Science:

Dean, School of Engineering and Applied Science

January 1991

ABSTRACT

Marvin W. Smith, Jr., Captain, USAF

Sediment Transport in Shallow Flow on an Impervious Surface

1991, 112 Pages

Master of Science (Civil Engineering)

University of Virginia

Sediment transport in the overland flow on an impervious surface has been studied to gain understanding of this process in shallow flow on a nonerodible boundary. Such a case occurs in stormwater flow over concrete and asphalt pavements of roads, parking lots and airports. The term sediment can include soil, rubber residue from aircraft tires, brake lining residue, paint flakes, and other particulate matter. Previous and current research has been reviewed in order to gain an understanding of the process of sediment transport. Existing mathematical models have also been reviewed in an attempt to find one which can be modified to give predictions on the transport of sediment in this case. Three velocity distributions (parabolic, logarithmic, and power) are employed with a varying sediment diameter to depth ratio in order to account for the effect of the sediment particle on the velocity distribution profile. The Shields diagram and previously established plots of the drag coefficient versus Reynolds number for a sphere are used to approximate the case of incipient motion of a particle in steady uniform and nonuniform shallow flow. An approximate, theoretically based mathematical procedure is derived to estimate this process. Appropriate simplifications, assumptions, or transformations have been made in order to achieve a solution to the model equation. The end result is a set of curves which relate the parameters of this particular sediment transport problem using a sediment transport efficiency parameter. Actual laboratory or field data is not available for this particular case of sediment transport and the resources were not available to obtain such data during this research. However, the presented model provides expected results using hypothetical data. The assimilation of actual numerical values for the efficiency parameter and a procedure to determine the total available sediment is left to others to achieve by field or laboratory means.

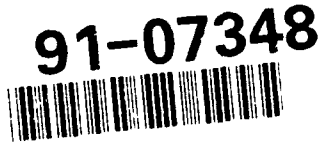

SEDIMENT TRANSPORT IN SHALLOW FLOW ON AN IMPERVIOUS SURFACE

Marvin W. Smith, Jr.

ABSTRACT

Sediment transport in the overland flow on an impervious surface has been studied to gain understanding of this process in shallow flow on a nonerodible boundary. Such a case occurs in stormwater flow over concrete and asphalt pavements of roads, parking lots and airports. The term sediment can include soil, rubber residue from aircraft tires, brake lining residue, paint flakes, and other particulate matter. Previous and current research has been reviewed in order to gain an understanding of the process of sediment transport. Existing mathematical models have also been reviewed in an attempt to find one which can be modified to give predictions on the transport of sediment in this case. Three velocity distributions (parabolic, logarithmic, and power) are employed with a varying sediment diameter to depth ratio in order to account for the effect of the sediment particle on the velocity distribution profile. The Shields diagram and previously established plots of the drag coefficient versus Reynolds number for a sphere are used to approximate the case of incipient motion of a particle in steady uniform and nonuniform shallow flow. An approximate, theoretically based mathematical procedure

is derived to estimate this process. Appropriate simplifications, assumptions, or transformations have been made in order to achieve a solution to the model equation. The end result is a set of curves which relates the parameters of this particular sediment transport problem using a sediment transport efficiency parameter. Actual laboratory or field data is not available for this particular case of sediment transport and the resources were not available to obtain such data during this research. However, the presented model provides expected results using hypothetical data. The assimilation of actual numerical values for the efficiency parameter and a procedure to determine the total available sediment is left to others to achieve by field or laboratory means.

ACKNOWLEDGEMENTS

I wish to thank Dr. B. C. Yen for his stimulation, advice, and continual assistance in the preparation of this thesis research. Dr. Yen's effort in this thesis work was much greater than advisement alone, and if it customary, his name would be added as co-author.

I would also like to express my thanks to the Air Force Institute of Technology (AFIT) whose Civilian Institute (CI) program and financial assistance made this work possible.

Finally, I am very thankful to my wife for her patience and encouragement.

TABLE OF CONTENTS

LIST OF FIGURES

NOMENCLATURE

A	Cross-sectional area of flow, normal to flow direction
A_b	Plan area of bed
A_p	Areal grain packing, or the ratio of the bed area covered by the grains to the total bed area
A_s	Cross-sectional area of sediment particle
A_s'	Area of channel bed covered by sediment particles
A_{sn}	Area of sediment particle surface normal to flow
A_{sp}	Surface area of sediment particle
a	Distance between particle center of gravity and point of support
d_s	Characteristic Diameter of sediment particle
F_D	Force of drag on a submerged sediment particle
F_g	Force of gravity on submerged sediment particle
F_L	Force of lift on a submerged sediment particle
F_p	Force of hydrostatic pressure on a submerged sediment particle
F_s	"Pushing" force on a submerged sediment particle caused by an adjacent sediment particle
F_{sx}	Force acting on a submerged sediment particle in x-direction
F_w	Submerged weight of the sediment particle
Fr	Froude Number
f	Weisbach's resistance coefficient
f_R	Coefficient of resistance due to rainfall
g	Gravitational constant
h	Depth of overland flow
i	Lateral input, such as rainfall
k	Surface roughness of channel bed, including

	any "roughness" caused by the formation of the sediment particles, an average over entire pavement area
L_o	Length of the overland flow
M_f	Momentum flux
M	Sediment deposition parameter
n	Manning's roughness factor
P	Wetted perimeter
P_s	Length of sediment particle circumference contacting bed
p	Pressure intensity
Q	Discharge of main flow
q	Volumetric flow rate per unit width
q_i	Lateral flow rate per unit length of channel
q_s	Volumetric sediment transport rate per unit width
q_{sd}	Dimensionless sediment transport rate
R	Hydraulic Radius
Re	Reynolds Number
S_w	Longitudinal slope of surface of flow
S_0	Pavement slope, the one-dimensional maximum gradient
S_f	Friction slope
S_e	Gradient of dissipated energy
SD	Size distribution of sediment particles
SF	Shape factor required to relate sediment particle shape to that of a sphere
s_q	Storage of sediment within control volume
T	Free surface width

U	Mean flow velocity
U_{cr}	Critical mean flow velocity required for incipient motion of the sediment particle
U_i	Mean velocity of lateral flow
U_s	Mean velocity of sediment particle
U_∞	Free stream velocity
u	Local temporal mean velocity of main flow
u_s	Local mean velocity of sediment particle
u_*	Shear velocity
V	Volume
V_s	Sediment particle volume
w	Settling velocity of a sediment particle
x	Longitudinal coordinate along channel bottom direction
y	Coordinate perpendicular to x on vertical plane
α	Kinetic energy correction factor
β	Momentum flux correction factor
β_s	Momentum flux correction factor for flow local to the sediment
γ	Specific weight of water
γ_s	Specific weight of sediment particle
δ	Boundary layer thickness
δ'^n	Nominal thickness of viscous sublayer
ζ	Parameter relating U_{cr} to drag force
Θ	Angle between bed and horizontal plane
K	Pressure correction factor
μ	Dynamic viscosity of water

ν	Kinematic viscosity of water
ξ	Sediment transport efficiency parameter
Π	Function
ρ	Density of water
ρ_s	Density of sediment particle
σ	Surface tension
τ_o	Average boundary shear stress
Φ	Sediment particle pickup parameter
ϕ	Angle of repose of submerged sediment particle
χ	Parameter universal to turbulent flow
ω	Sediment particle weight parameter

1. INTRODUCTION

The modeling, and hence control, of overland flow has been a widely studied engineering problem for many hundred years. The study of erosion, deposition, scour and related problems is almost as old. However, the fairly recent environmental "awakening" by the world's peoples is forcing the engineering profession to study the less visible and more unknown aspects of overland flow. One such aspect is sediment as a pollutant carrier. Although, the problem of sediment as a pollutant and the control of sedimentation by stormwater runoff has gained public attention and regulation in general, the stormwater transport of pollutants for special situations still requires much attention. This is especially true in the case of pollutant transport by sheet flow across parking lots, airfields and other paved areas into groundwater, streams and rivers.

Numerous equations and methodologies exist to calculate and/or estimate sediment transport caused by overland flow on agricultural and construction sites, and sedimentation in rivers, streams, pipes and channels. However, little research has addressed the hydraulics of sediment transport by nonuniform sheet flow over a nonerodible impervious boundary, such as a pavement.

The scope of this investigation is to apply dimensional analysis, physical theory, and previously established knowledge on fluid mechanics and sediment transport to the

case of particle transport by overland flow on a nonerodible impervious boundary. The research is limited to the case similar to shallow flow normally encountered as stormwater runoff on airfield pavements. Considering the given case and further restricted by the lack of physical understanding and field data, the objective of this study is to determine the form of a particle transport equation which can be applied to the conditions of shallow flow over an impervious surface. This transport is an approximate model given the simplifications required for development. Future research is required to further verify the model. The model applies to particulate matter only and is not capable of simulating transport of oils, fibrous material, or dissolved pollutants. However, future models could account not only for the transport of sediment but also other pollutants by the use of a concentration multiplier. Those pollutants in dissolved form would be accounted for by considering their adsorption to the sediment particles.

2. REVIEW OF RELATED LITERATURE

2.1 BACKGROUND

Most of the previous research in sediment transport has been confined to the cases of agricultural erosion and river and reservoir sedimentation and erosion. The case of agricultural erosion greatly differs from the case studied here mainly due to the presence of an erodible boundary and non-plane flow (i.e. rills). The flow depths and regime encountered in river and reservoir erosion and sedimentation make previous research in that area of limited value for sediment transport by shallow flow on a plane, nonerodible surface. However, much literature concerning the above two cases has been reviewed and applicable ideas and methods have been applied in this research. The literature review was divided into two areas to simplify discussion: hydraulics of overland flow and the mechanics of sediment transport.

2.2 HYDRAULICS OF OVERLAND FLOW

A literature review of relevant fluid mechanics and hydraulics was accomplished in order to establish a sound foundation for this research. The texts of Chow (1959) and Shames (1982) were particularly helpful in this regard.

The literature review on hydraulics was divided into

three areas: the study of shallow open channel flow, the description and measurement of resistance to flow, and the description and measurement of the velocity distribution.

2.2.1 Shallow Open Channel Flow

One-dimensional shallow open channel flow can be described mathematically by the Saint-Venant equations which were first developed by Barre de Saint-Venant in 1871. The Saint-Venant equations are known as the shallow water wave equations and can be expressed in terms of discharge or velocity. These shallow water equations are composed of the continuity equation (based on the principle of conservation of mass) and either the momentum or energy equation (based on Newtons' second law of motion). The equations apply for both laminar and turbulent flow. Researchers use this combination of equations to describe shallow water flows, including overland flows.

Rouse and McNown (1945) provide an interpretation of the energy and momentum principles in hydraulics. Various researchers have provided discussion on the differences between the use of the energy and momentum equations. Yen and Wenzel (1970) provide a detailed discussion of both the momentum and energy approach and the correlation between the two. They also provide a good

review of past research on equations for steady spatially varied flow. The application of the Saint-Venant equations to the modeling of the rainfall-runoff process is discussed by Yen (1986).

Steady uniform or nonuniform flows have been studied and are presented for the laminar, transition, and turbulent regimes. Unsteady uniform flow rarely occurs in nature and is not discussed.

2.2.1.1 Steady Uniform Flow

The velocity of a steady uniform flow is usually expressed by either the Manning, Chezy, or Weisbach formulas. The Manning formula is

$$U=\frac{1.49}{n}R^{2/3}S^{1/2} \qquad (2.1)$$

where n = Manning's coefficient of roughness,

U = mean velocity,

R = hydraulic radius,

S = slope of the energy line.

Given the geometry of the flow and q (or U and h), Manning's n can be found. Therefore, n is no longer an independent variable but could be used to replace either U, q, or h. However, this is impractical to do so and since n varies

considerably with depth, its use is not proper in shallow flow conditions. Therefore, the use of n has no advantage for the flow conditions studied in this thesis.

The Chezy formula is

$$U=C\sqrt{RS} \tag{2.2}$$

where C = Chezy's factor of flow resistance.

The Weisbach formula is

$$U=\sqrt{\frac{8}{f}g}\ \sqrt{RS} \tag{2.3}$$

where g = gravitational constant,

and f = Weisbach resistance coefficient.

The state of steady flow can range from laminar to turbulent. Normally, the relationship between the Weisbach f and the Reynolds number (Re=UR/ν) is used to express the state of flow resistance for uniform and nearly uniform flows (Chow, 1959). The Weisbach equation can be written as

$$f=\frac{8gRS}{U^2} \tag{2.4}$$

In the laminar flow range with Re < 500,

$$f=\frac{24}{Re} \qquad (2.5)$$

The Blasius equation expresses the f-Re relationship for smooth pipes as (Chow, 1959)

$$f=\frac{0.223}{Re^{0.25}} \quad for \quad 750 \le Re \le 25,000 \qquad (2.6)$$

The von Karman-Prandtl expression for higher Reynolds numbers for a smooth surface is

$$\frac{1}{\sqrt{f}}=2\log(Re\sqrt{f})+0.4 \qquad (2.7)$$

And for a hydraulically rough boundary

$$\frac{1}{\sqrt{f}}=2\log(\frac{R}{k})+2.16 \qquad for \ \frac{Re/\sqrt{f}}{R/k} > 50 \qquad (2.8)$$

where k = the Nikuradze equivalent roughness size. These equations are often used for open channel flow. From Eqs. 2.1 to 2.3, Weisbach's f, Chezy's C and Manning's n can be related by

$$\sqrt{\frac{8}{f}}=\frac{C}{\sqrt{g}}=\frac{1.49}{\sqrt{g}n}R^{1/6} \qquad (2.9)$$

2.2.1.2 Steady Nonuniform Flow

The equation for steady nonuniform flow with lateral discharge or spatially varied flow is often solved for the slope of the flow surface (Yen and Wenzel, 1970). The momentum equation is

$$\frac{dh}{dx} = \frac{S_0 - S_f + \frac{q}{gA}(U_q \cos\phi - 2\beta U) - \frac{U^2}{g}\frac{d\beta}{dx}}{\cos\theta - \frac{\beta U^2}{gD}} \qquad (2.10)$$

and the energy equation is

$$\frac{dh}{dx} = \frac{S_0 - S_e + \frac{q}{gA}(\frac{U^2 q}{gA} - \frac{3\alpha U^2}{2g} + H_{pL} - h\cos\theta) - \frac{U^2}{2g}\frac{d\alpha}{dx}}{\cos\theta - \frac{\alpha U^2}{gD}} \qquad (2.11)$$

where h = depth of flow,

A = flow cross-sectional area,

D = hydraulic mean depth = A/(water surface depth),

x = longitudinal direction,

S_0 = bed slope,

S_f = friction slope,

S_e = energy loss slope,

θ = angle of the bed with horizontal datum,

β = momentum correction coefficient,

α = energy correction coefficient,

q = lateral flow rate per unit length of channel, negative for outflow,

U_q = lateral flow velocity when joining the main flow with an angle ϕ.

If there is no lateral flow and the variation of β or α with x is small, Eqs. 2.10 and 2.11 can be simplified, respectively, as

$$\frac{dh}{dx} = \frac{S_0 - S_f}{\cos\theta - \frac{\beta U^2}{gD}} \tag{2.12}$$

and

$$\frac{dh}{dx} = \frac{S_0 - S_e}{\cos\theta - \frac{\alpha U^2}{gD}} \tag{2.13}$$

2.2.2 Resistance to Flow

Resistance to flow is characterized by three types; skin friction, form resistance, and wave resistance. Skin friction is usually the dominate resistance to flow in open channels over nonerodible boundaries. This skin friction results from the flow of fluid over the channel bed and around sediment particles. In the case of an alluvial

river, form drag may also become important in the presence of bed forms such as ripples, dunes or anti-dunes. Wave drag may become important in high Froude number flow, in nonlinear channel alignment, and in very shallow flow around a large particle where significant wave height is formed.

The open-channel flow equations contain various parameters to describe the resistance to flow. Rouse (1965) provides a form for the rate of the cross-sectional resisting force and states that the resistance coefficient in Weisbach form, f, is a function of the Reynolds number, the relative roughness, the cross-sectional shape, the non-uniformity of the channel in both profile and plan, the Froude number, and the degree of unsteadiness. The first three variables represent the effect of surface resistance, the next two represent the effect of form and wave resistance, and the last represent the effect due to local acceleration.

The resistance coefficients for a steady, spatially varied flow are discussed and differentiated in a helpful paper by Yen, Wenzel and Yoon (1972). The friction resistance term found in the shallow water equation is the friction slope, S_f. This term is found in the equation derived by using the momentum approach, whereas the gradient of dissipated energy, S_e, is used in the energy derived equation. The resistance coefficient, f, is found as a function of either the friction slope, S_f, or the gradient

of dissipated energy, S_e. For gradually varied flow, Yen, Wenzel and Yoon (1972) describe the friction coefficient as a function of the Reynolds number, Froude number, the relative roughness, the cross-sectional shape, the non-uniformity, and the relative mass, momentum, and energy inputs of the lateral flow.

Because of the difficulties involved, the friction coefficient is often computed from the Weisbach, Manning, or Chezy equations which were developed for steady uniform flow. Experiments on the variation of f due to impediments to the flow (such as grasses or clumps of soil) have been studied by many. Examples include Chen (1976) and Sadeghian (1990). Podmore and Huggins (1980) used laboratory experiments to develop a relationship between the physical roughness of the flow area to hydraulic roughness coefficients.

The value of f is also greatly affected by raindrop impact. Woo and Brater (1962) gave the result of an experimental study. Yu and McNown (1964) used the gradually varied flow equation and data from the Army Corps of Engineers Los Angelos District to estimate the effect of rainfall on the Weisbach resistance coefficient. Yen et al. (1972) and Shen and Li (1973) further expanded on the raindrop effects.

Engman (1986) gives values for many roughness coefficients and discusses how the coefficients include the

effect of raindrop impact, channelization of flow, obstacles in the flow path, and other factors. Rouse, Koloseus, and Davidan (1963) describe f as a function of Reynolds Number, channel shape, and the ratio of bed roughness to flow depth.

2.2.3 Velocity Distributions

A wide open channel is one in which the width is greater than 10 times the depth of flow (Chow, 1959). In such cases, the velocity distribution in the center of the channel is not affected by the sides of the channel. Therefore, the velocity distribution can be considered as two-dimensional. Such will be considered the case in this work. As described by Chow (1959), the velocity distribution is generally nonuniform over the flow cross section. Therefore, in the one-dimensional formulation a coefficient must be used to correct for the velocity head which is usually greater than that computed by $U^2/2g$. When the energy principle is used, the coefficient is α, also referred to as the Coriolis coefficient. The velocity head is then computed as $\alpha U^2/2g$ and usually α ranges from 1.03 to 1.4.

When the momentum principle is used, a correction coefficient β is used which is also referred to as the Boussinesq coefficient. The value of β commonly ranges from

1.01 to 1.12. For a two-dimensional flow,

$$Uq\beta = \int_0^h u^2 \, dy \qquad (2.14)$$

where u = the local velocity component in the x-direction,

and q = h U.

For a three-dimensional flow,

$$U^2 A\beta = \int_A u^2 \, dA \qquad (2.15)$$

The momentum coefficient is also defined and discussed in a more rigorous manner by Yen (1973).

2.2.3.1 Laminar Flow

The velocity distribution in a steady uniform laminar flow is usually described by a parabolic equation

$$\frac{u}{u_h} = \left(\frac{2y}{h} - \frac{y^2}{h^2}\right) \qquad (2.16)$$

where u = point velocity of the flow,

u_h = velocity at the water surface,

y = distance normal to bed,

h = flow depth.

The mean velocity is found as

$$U=\frac{2}{3}\,u_h \qquad (2.17)$$

2.2.3.2 Turbulent Flow

Figure 2.1 describes the velocity distribution of a typical turbulent flow. As described by Robeson and Crowe (1985), the velocity in the viscous sublayer can be described by

$$\frac{u}{u_*}=\frac{u_* y}{\nu} \qquad (2.18)$$

where u_* = shear velocity,

ν = kinematic viscosity of the fluid.

The velocity in the turbulent zone is often described by the dimensionless, logarithmic, universal velocity-distribution law (Schlichting, 1968):

$$\frac{u}{u_*}=\frac{1}{\chi}\left(\ln\frac{y u_*}{\nu}+K\right) \qquad (2.19)$$

where χ = a parameter universal to turbulent flow and is independent of the nature of the wall.

Experimentally, χ=0.4 (Schlichting, 1968). The value of K depends upon the nature of the wall. The common form of the logarithmic velocity distribution in turbulent flow over a

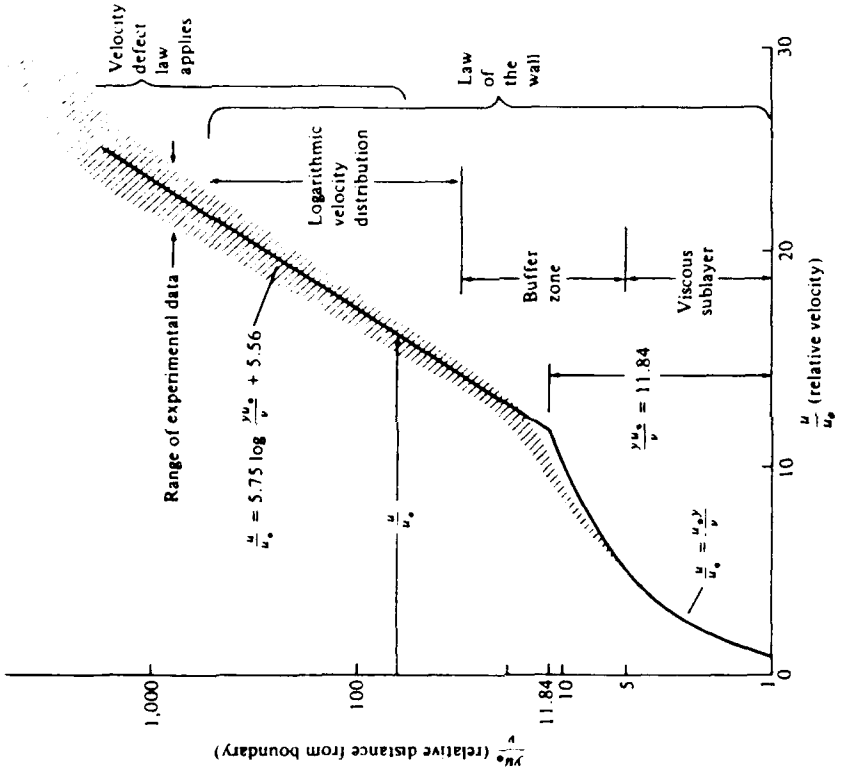

Figure 2.1 Velocity Distribution in a Turbulent Boundary Layer (from Robeson and Crowe, 1985)

smooth boundary is

$$\frac{u}{u_*}=5.75\log\left(\frac{u_* y}{\nu}\right)+5.5 \qquad (2.20)$$

A similar equation is used for turbulent flow over a rough boundary

$$\frac{u}{u_*}=5.75\log\left(\frac{y}{k}\right)+8.5 \qquad (2.21)$$

where k = the roughness of the channel bed.
The equation for a rough boundary is valid for $ku_*/\nu > 70$. Flow is said to be hydraulically rough when projections of the channel bed are fully exposed to the turbulent flow. This requires the viscous sublayer to be smaller than the height of the projections.

The region $30 \leq yu_*/\nu \leq 500$ is the upper portion of the law of the wall where the fluid viscosity is most important in the development of the velocity profile (Robeson and Crowe, 1985). In the buffer zone where $5 \leq yu_*/\nu \leq 30$ the velocity can neither be described by the viscous sublayer distribution nor the logarithmic distribution. It is often assumed the velocity distribution of the viscous sublayer extends to the point of nominal

thickness of the viscous sublayer, $\delta_n' = 11.84\upsilon/u_*$ (Robeson and Crowe, 1985).

Alternately, a power law has been used to represent the velocity distribution,

$$\frac{u}{u_h} = \left(\frac{y}{h}\right)^{\frac{1}{m}} \qquad (2.22)$$

It has been suggested that m = 6 corresponds to Manning's formula, m = 7 corresponds to Blasius' and m = 12 to the formula of Hazen-Williams.

2.3 MECHANICS OF SEDIMENT TRANSPORT

Sediment transport, long a topic of research in regard to erosion, siltation, and river sediment yield, is becoming a current topic of research in regard to shallow water flow. However, existing literature is not directly related to shallow flow although several approaches and fundamental findings are applicable.

One of the most well-known researchers in the area of sediment transport is A. Shields (1936). His plot (Figure 2.2) of the dimensionless shear stress versus the boundary shear Reynolds number is used to predict the initiation of sediment motion. However, Shields' (1936) work is limited because it does not predict deposition since the critical

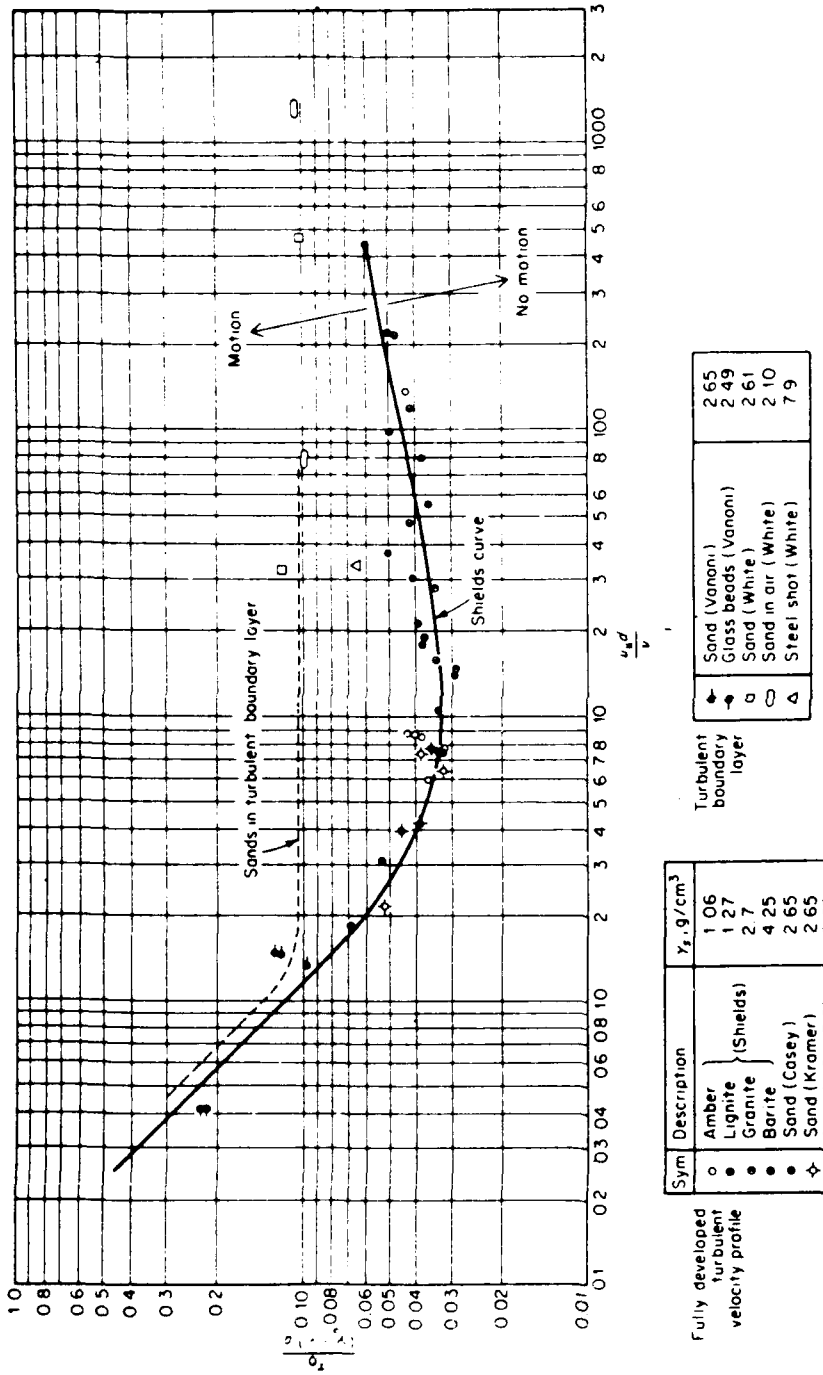

Figure 2.2 Shields Diagram

(from Graf, 1984)

velocity required to pick-up a particle is different from that required for deposition. Also, the Shields curve was developed for steady uniform turbulent flow with a small sediment particle size to depth ratio (d_s/h). Its applicability to nonuniform and unsteady flows with a large d_s/h should be further investigated.

MacDougal (1933) used flume experiments at the Massachusetts Institute of Technology to derive a sediment transport equation for bedload which varied with bed slope, flow discharge, and critical flow discharge at which transport began. The variable of mean bed shear stress appeared to be the best to describe sediment transport for several flume experiments by Stein (1965). However, the depths of flow in these experiments were all greater than 0.4 ft.

Rottner (1959) used dimensional analysis to develop a sediment transport model for bedload. The particle size to depth ratio, d_s/h, was recognized as an important parameter. Flow depth and velocity were also used to compute the discharge; however, slope was not included.

Bagnold (1966) approached the sediment transport problem from general physics. Energy balance and mechanical equilibrium considerations were used to develop the model which related a sediment transport rate to a stream power function. Yang (1973) stated that unit stream power is the dominant factor to determine the initiation and total

sediment discharge for an alluvial channel under equilibrium conditions.

Ackers and White (1973) used a combination of dimensional analysis and physics to develop a sediment transport equation for steady uniform flow. Their dimensionless sediment transport parameter is described as a function of a dimensionless mobility number and a dimensionless grain diameter. They found that the transport of fine material was most related to shear velocity, whereas the transport of coarse material is most related to mean velocity of flow. The authors stated that their work does not apply for cases where the Froude number is less than 0.8.

Previous sediment transport laboratory data was compiled and reviewed by Cooper (1970), Cooper et al. (1972), and Brownlie (1985). Since most sediment transport formulas are empirical or semi-empirical and developed from laboratory flume data, the authors were concerned with the dangers of engineers extrapolating the equations to field use. Most of the laboratory data concerned a flow depth in the range of h/d_{s50} from 10 to 10,000. The term d_{s50} refers to sediment particle diameter of which 50% of the particles are finer. Only 1% of the laboratory data was collected for flows with $h/d_{s50} < 7$. Also, many previous data was collected with flows having a large Froude number whereas the case of shallow, slow flow might have a Froude number of

0.3. All of the data was collected for the alluvial channel case where the bed is erodible and the supply of sediment is infinite, the Reynolds number is high, and the geometry is not similar. Therefore, the alluvial channel data is not used to verify the model presented in this work even though some of the data has a d_s/h ratio in the same range.

Vanoni (1984) provides a thorough review of the history of sediment transport study. Texts that are helpful in a study of sediment transport include Graf (1984), Simons and Şentürk (1976), and the ASCE Sedimentation Engineering Manual, edited by Vanoni (1977).

An early study of the effect of the shape of a particle on its fall velocity was conducted by Albertson (1953). Gravel particles were studied and the author suggested that the nominal diameter of the sediment particle should be used when calculating Reynolds number and drag coefficient. The nominal diameter is the diameter of a sphere having the same volume. This work has been cited by many researchers studying sediment transport in flows where the depth is much greater than the particle size and the particle terminal velocity is an important parameter.

2.4 APPLICABILITY OF REVIEWED LITERATURE TO THE STUDIED CASE

Applicable data was not found to calibrate and verify the

model presented later in the thesis. Even data on shallow flow with no sediment is scarce. The Shields diagram is the only experimental data that can be used as an approximation. The two most important aspects of sediment transport by shallow flow are lower Reynolds number and large d_s/h ratio. These two factors distinguish the case here from that generally studied previously. Therefore, sediment transport relationships based on flows with small particle size to flow depth ratio, such as encountered in rivers and most flume studies, are most likely not applicable to this study. Also, theories and ideas associated with flow of high Reynolds numbers are not applicable. This includes the region of constant Weisbach resistance coefficient at high Re values.

Previous studies of sediment movement in turbulent flows have indicated that particles are most often put into motion by the "gusting" effect of the turbulent flow. This is known as the "bursting phenomenon." Since the shallow flow is characterized by lower Reynolds number, the flow is usually laminar or in the transition range. Therefore, the flow is unlikely to be "gusting" and the particles are not put into motion by the "bursting phenomenon". Instead, the wake produced behind the particle by the flow is the primary inducement to particle movement. Since the particle size to flow depth ratio is large, the particles will most likely move by translation or rotation rather than by lifting into

the flow.

3. DIMENSIONAL ANALYSIS

The general case of sediment transport by overland flow is a complex process which has not been satisfactorily addressed by the engineering profession. Rigorous analytical solutions are not available. Sediment transport by steady uniform flow has been studied by several researchers as indicated in the previous section. Because of the complexity and nature of the problem, all have made many and varied simplifications to achieve the final form of the model. However, many great differences exist between the previous work and the focus of this thesis. The major difference is the lack of an erodible bed in the case of flow on an impervious surface such as airfield pavement. Also, higher Reynolds numbers will not be encountered in shallow flow and the d_s/h ratio will be much greater. Therefore, two approaches have been used here in order to study the problem of sediment transport by overland flow on an impervious surface. The first approach is the use of dimensional analysis and the second is an approach from general physics.

Figure 3.1 can be used to represent the sediment transport process for the case studied here. A two-dimensional case is considered and any variances in the cross-section are ignored.

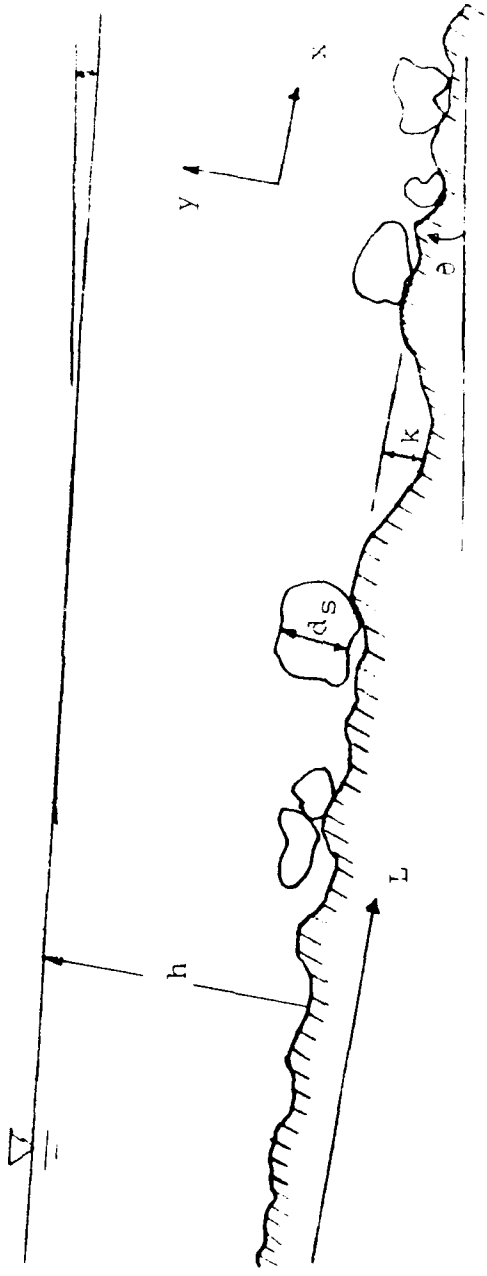

Figure 3.1 Definition Sketch of Flow with Particles

3.1 DETERMINATION AND DEFINITION OF SYSTEM VARIABLES

The focus of this study is to arrive at an expression for q_s, the volumetric sediment transport rate (per unit width) for a two-dimensional shallow water flow. Therefore, for the general case of initially "clear" steady flow with a very wide channel and uniform density, cohesionless sediment particles with no lateral input of flow and no upstream or lateral input of sediment, this rate can be expressed as:

$$q_s = \Pi_1(\mu,\rho,\gamma,\sigma,\rho_s,d_s,SF,SD,A_p,\tau_0,S_0,h,U,L_o,\beta) \qquad (3.1)$$

where Π represents a function. The above variables have been grouped into the three categories of Fluid, Sediment, and Flow.

Fluid variables are;

μ = dynamic viscosity,

ρ = density,

γ = specific weight,

σ = surface tension.

Sediment variables are;

q_s = volumetric transport rate per unit width (the dependent variable sought),

ρ_s = sediment particle density,

d_s = representative sediment diameter,

SF = shape factor,

SD = size distribution,

A_p = available sediment on the bed expressed as areal grain packing or the ratio of the area of the particles to the total area of the channel bed in the flow segment (Note: the number of grains is a function of A_p/d_s^2).

Steady uniform flow variables are;

S_0 = channel bed slope in the direction of flow,

h = depth of flow,

U = cross-sectional mean velocity of flow,

β = momentum flux correction factor due to a nonuniform flow distribution over the cross section,

L_o = length of flow segment,

τ_0 = average boundary shear stress

3.2 SINGLE PARTICLES IN STEADY UNIFORM FLOW

The sediment transport function of Eq. 3.1 is arranged into a nondimensional form with the use of dimensional analysis and the dimensions of Length (L), Mass (M), and Time (T) of the variables as shown below:

	ρ	d_s	U	μ	γ	σ	q_s	ρ_s	SF	SD	A_p	h	L_o	S_0	β
L	-3	1	1	-1	-2	-2	3	-3	0	0	1	0	1	0	0
M	1	0	0	0	1	1	0	1	0	0	0	0	0	0	0
T	0	0	-1	-1	-2	0	-1	0	0	0	0	0	0	0	0

Note that for the case of steady uniform flow τ_0 =

$\gamma h S_0$. Since all other parameters are considered, τ_0 is redundant and can be ignored. Selecting ρ, h, and U as repeating variables, Eq. 3.1 can be expressed in a nondimensional form as:

$$\frac{q_s}{hU}=\Pi_2\left(\frac{Uh\rho}{\mu}, \frac{\rho U^2}{\gamma h}, \frac{U^2 h\rho}{\sigma}, \frac{\rho_s}{\rho}, \frac{d_s}{h}, SF, SD, \frac{L_o}{h}, A_p, S_0, \beta\right) \qquad (3.2$$

where $\rho hU/\mu$ = Reynolds Number (Re),

$\sqrt{U^2\rho/(h\gamma)} = U/\sqrt{gh}$ = Froude Number (Fr),

g = gravitational acceleration,

$U^2h/(\sigma/\rho)$ = Weber number (Wb).

Replacing ρ_s/ρ with $(\rho_s/\rho)-1$ and multiplying $[(\rho_s/\rho)-1]$ by the dimensionless terms $hU\rho/\mu$ and $\gamma h/U^2\rho$ gives

$$[(\rho_s/\rho)-1](\gamma h/U^2\rho)/(\mu/hU\rho) = [(\rho_s/\rho)-1]\gamma h^2/\mu U,$$

which can be represented by w/U, where w is the terminal fall velocity of the particle. Therefore, Eq. 3.2 can be expressed alternately as:

$$\frac{q_s}{hU}=\Pi_3\left(Re, Fr, Wb, \frac{d_s}{h}, \frac{w}{U}, SF, SD, A_p, \frac{L_o}{h}, S_0, \beta\right) \qquad (3.3)$$

Many different combinations of these parameters are possible. However, the above are considered appropriate in this study. Many of the these combinations have been used in previous researches. For example, the shear Reynolds

parameter $u_*h\rho/\mu$ introduced by Shields (1936) can be given as $Re\sqrt{\tau_0/\overline{U^2}\rho}$ where $u_*=\sqrt{\tau_0/\rho}$ is defined as the bed shear velocity.

3.3 DETERMINATION OF SIGNIFICANT DIMENSIONLESS PARAMETERS

Although all of the above parameters apply to the case of transport of uniform density, cohesionless sediment particles in initially "clear" steady flow in a wide overland surface or channel, a useable relationship cannot be established with such a large number of parameters. That is, some parameters must be combined or eliminated through assumptions or simplifications to reduce the total number of parameters to a manageable amount. In order to prioritize the above nondimensional parameters, each is summarized below:

Dimensionless Parameter	Conditions When the Parameter Most Affects Sediment Transport
Re	The ratio of the inertia force to the viscous force. Important for shallow depth or low velocities, i.e. laminar flow and transitional developing turbulent flow which is usually

	the case for overland and pavement flows. Also important to show the effect of temperature changes on the flow.
Fr	Ratio of the inertia force to the force of gravity. Without surface wave distortion, it is not important when the flow is subcritical with Fr < 0.5.
Wb	The surface tension effect is expected to be unimportant unless the amount of water is so small that a continuous sheet flow cannot be sustained and the flow is broken into small pots, which, if this ever occurs, it will only be at the upstream end of the overland surface.
d_s/h	It reflects the particle size as an obstacle to the flow. When its values is small, it merely reflects the surface roughness of the bed. When d_s is about one-quarter of depth or more, it also reflects the disturbance

	of the particle to the flow velocity distribution.
w/U	The relative mobility of the particle in water. Since the flow depth is small, the particle is never able to reach terminal fall velocity, w. In the case of a constant ρ_s/ρ, this parameter is not significant in shallow flow and w is used only as a sediment property indicator. However, this parameter is useful in the study of nonuniform flow since it is related to the bed shear τ_0 and bed slope S_0.
SF	The shape of the particle affects the drag force. Thus, SF is most important when the shape is far from spherical, e.g. a disk normal to the flow. For normal sand-gravel type sediment, the significance of this parameter is only of secondary importance.
SD	Significant only for greatly varying particle sizes. Equal to zero for uniform particle sizes.

L_o/h	Since this term expresses the length of the flow channel where sediment can be picked up, it must be considered for the calculation of sediment transport.
A_p	Most important when the sediment density is sparse. For densely packed particles such as in alluvial channels, the sediment packing density becomes statistical.
S_0	The channel bed slope reflects significance of bed shear, and thus, the ability of the flow to move the bed particles.
β	When the velocity distribution is highly nonuniform and varying with the flow distribution. Normally, in cases of a large flow depth to sediment particle size, the effect of this parameter parameter is small. However, this is not the case here.

Using the above evaluations, for a steady uniform,

shallow, subcritical flow on an impervious pavement of small slope with nearly spherical constant density sediment on it, the dimensionless independent parameters in Eq. 3.3 can be prioritized into primary and secondary importance categories as follows:

Primary Parameters	Secondary Parameters
$Re, d_s/h, L_o/h, A_p, S_0, \beta$	Fr, w/U, SF, SD, Wb

Thus, Eq. 3.3 can be reduced to

$$\frac{q_s}{hU} = \Pi_4 \left(Re, \frac{d_s}{h}, A_p, \beta, S_0, \frac{L_o}{h} \right) \qquad (3.4)$$

If $q_s/q_{s\ max}$ versus flow length, L, were plotted, the maximum sediment transport rate is achieved after a finite distance and does not increase with additional downstream distance. Since q_{smax} would be difficult to determine, L_x is defined as the flow length corresponding to a sediment transport rate which is x% of the maximum transport rate. L_x will be referred to as the threshold value of L, flow length. Above a value corresponding to L_{90}, the sediment transport rate is almost independent of L_o and hence L_o/h. The actual value of x could be set as 95, 98, or some other meaningful level.

A dimensional analysis is accomplished in the same manner as that for q_s in order to develop the function for

U_{cr}, the critical flow velocity required for incipient motion of the sediment particle. Neglecting the terms σ, SF, SD, A_p, and L_0, the dimensionless relationship for critical velocity is

$$\frac{U_{cr}}{\sqrt{gd_s}} = \Pi_5 \left(\frac{d_s}{h}, \beta, Re_c, S_0, \frac{\rho_s}{\rho} \right) \tag{3.5}$$

where $Re_c = (U_{cr} h \rho)/\mu$,

$U_{cr}/\sqrt{gd_s} = (\rho U_{cr}^2)/(\gamma d_s)$.

For both above cases, steady nonuniform flow can be represented by

$$\frac{q_s}{hU} = \Pi_5 \left(Re, \frac{d_s}{h}, A_p, \beta, S_0, \frac{L_o}{h}, \frac{\tau_0}{\rho U^2} \right) \tag{3.6}$$

where $\tau_0/\rho U^2$ is used to represent the dimensionless bed shear and accounts for the nonuniformity of the flow.

In order to consider the effect of rainfall on the sediment transport rate, other parameters must by included. As given by Yoon and Wenzel (1971), the dimensionless relationship for spatially varied flow is

$$\frac{\tau_0}{\rho U^2} = \Pi_6 \left(Re, Fr, \frac{\rho i h}{\mu}, Fr_R, \frac{\rho i d_R}{\mu}, \frac{\epsilon}{h}, S_0, \eta, \lambda \right) \tag{3.7}$$

where Fr_R = Froude number of the rainfall,

i = rainfall intensity,

ϵ = boundary roughness,

η = raindrop pattern parameter,

λ = raindrop shape parameter.

The case of unsteady flow can be represented by including a term to account for the variation of the flow depth with time. The general case would include all of the above considerations.

4. THEORETICAL CONSIDERATIONS

The sediment transport model is developed by reviewing physical considerations and comparing the outcome of this review with the results from dimensional analysis. Past developments in sediment transport technology are modified for the case of shallow flow over an impervious surface. Modifications are necessary to account for the shallow flow depth to particle diameter ratio and also to reflect both a laminar and turbulent velocity distribution.

First, the particle mobility problem is addressed from general physics. The first procedure is a definition of all forces acting on a particle and the critical condition when the particle is about to move. The second procedure is the application of Newton's law of motion to a sphere.

4.1 FORCES ON SUBMERGED SINGLE PARTICLES

4.1.1 Steady Uniform Flow

Figure 4.1 depicts a particle at rest on a plane bed submerged under steady uniform flow. Incipient motion is described as the point at which the particle is just about to move if any additional force, however small, is applied. Once this additional force is applied, the particle will

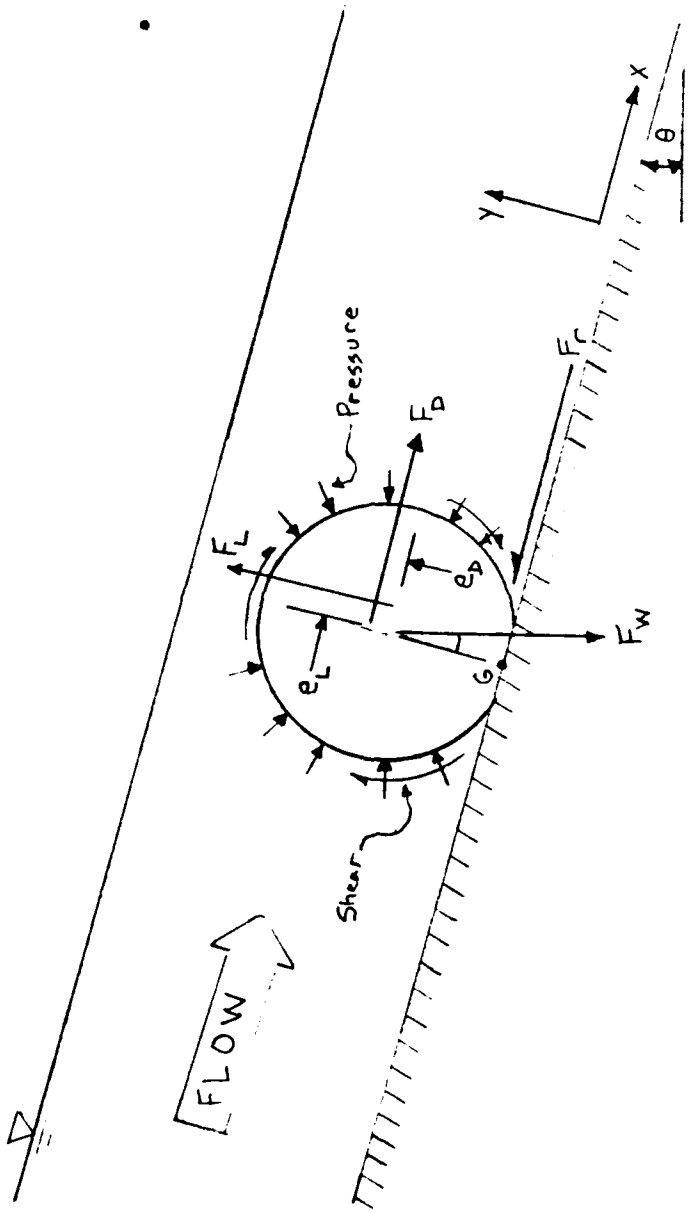

Figure 4.1 Forces on a Submerged Particle in Steady, Uniform Flow

move by any one or a combination of three means; lifting, sliding, or rotating.

Forces acting on the particle in Figure 4.1 include drag, lift, weight, and resistance. The drag and lift forces are due to the flow surrounding the particle. The weight force is the submerged weight of the particle in the fluid. Resistance is the friction force acting between the particle surface and the bed surface. The drag, lift, weight, and resistance forces can be described by the following equations:

$$Drag: \quad F_D = C_D \frac{U_r^2}{2} A_{sn} \tag{4.1}$$

$$Lift: \quad F_L = C_L \frac{U_r^2}{2} A_{sn} \tag{4.2}$$

$$Weight: F_w = (\gamma_s - \gamma) V_s = (\rho_s - \rho) g V_s \tag{4.3}$$

$$Resistance: F_r = C_\mu (F_{wy} - F_L) \tag{4.4}$$

where A_{sn} = the projected area of the particle normal to the direction of flow,

C_D is the drag coefficient,

C_L is the lift coefficient,

U_r is a reference velocity which can be related to the approaching flow velocity, U, along the x-direction passing through the particle's center of

gravity, G, and a coefficient C_μ, i.e.,

$U_r = C_\mu U^2$, V_s is the volume of the particle,

and C_μ is a nominal friction coefficient.

The coefficient C_u is a function of the momentum flux correction factor, β.

Lift occurs when the lifting force, F_L, is greater than the submerged weight of the particle in the y-direction, F_{wy}. The case of incipient motion by lifting is

$$F_L - F_{wy} = 0 \tag{4.5a}$$

or

$$C_L \frac{\rho C_u U^2}{2} A_{sn} = (\rho_s - \rho) g V_s \cos\theta \tag{4.5b}$$

Solving for the incipient motion critical mean velocity, U_{cr}, provides

$$U_{cr}^2 = \left(\frac{\rho_s}{\rho} - 1\right) g \frac{K_1}{C_\mu C_L} \cos\theta \sqrt{d_s} \tag{4.6}$$

where $K_1 = 2V_s/A_{sn}$ is a function of the geometry of the particle and is equal to 8/3 for a sphere.

The lift coefficient C_L is a function of the Reynolds number of the flow around the particle ($Re = Ud_s/\nu$). The coefficient C_u is a function of the momentum correction coefficient over the depth of the particle, β_s,

$$\beta_s = \frac{\int_0^{d_s} u^2 \, dy}{U_r^2 \, d_s} \qquad (4.7)$$

where U_r = a reference velocity of the flow.

Hence, for a constant θ, U_{cr} can be expressed

$$U_{cr} = K_L(\beta_s, Re)\sqrt{d_s} \qquad (4.8)$$

where K_L = a function of β_s and Re.

For the airfield case, pavement slopes range from 2% to 7%. Therefore, θ ranges from approximately 1.15 to 4.01 degrees, and $\cos\theta \sim 1$, $\sec\theta \sim 1$, and $\tan\theta \sim \sin\theta = S_0$.

The particle will slide along the bed surface when the resultant force applied by the flow in the x-direction is positive. The incipient case of translation is

$$F_D + F_W \sin\theta - F_r = 0 \qquad (4.9)$$

Substituting Eqs. 4.1 to 4.4 into Eq. 4.9 and solving for the incipient motion critical velocity,

$$U_{cr} = \left[\frac{(C_\mu \cos\theta - \sin\theta)}{C_u (C_D + C_\mu C_L)} \left(\frac{\rho_s}{\rho} - 1 \right) g K_1 d_s \right]^{\frac{1}{2}} \qquad (4.10)$$

Therefore,

$$U_{cr}=K_D(\beta_s, Re, C_\mu)\sqrt{d_s} \qquad (4.11)$$

where K_D = a function.

Even if the particle does not move by lifting or sliding, it can still be transported by rotating or rolling along the bed. This would occur when the forces exerted in the x-direction about the support point of the particle create sufficient torque to overcome the resisting torque (Figure 4.2).

The incipient case is

$$F_D e_D - F_L e_L + F_w \frac{d_s}{2}\tan\theta = 0 \qquad (4.12)$$

The moment arms e_D and e_L are a function of the particle geometry and flow velocity around it, and hence, are a function of β_s. Therefore, by substituting Eqs. 4.1 to 4.3 into Eq. 4.12, the critical velocity can be expressed as

$$U_{cr}=K_I(\beta_s, Re)\sqrt{d_s} \qquad (4.13)$$

In each incipient case of lifting, sliding, or rolling, the critical condition is expressed in terms of U_{cr}, the critical approaching flow velocity in the x-direction passing through the center of gravity of the particle. The main observation from the above physical view is that the

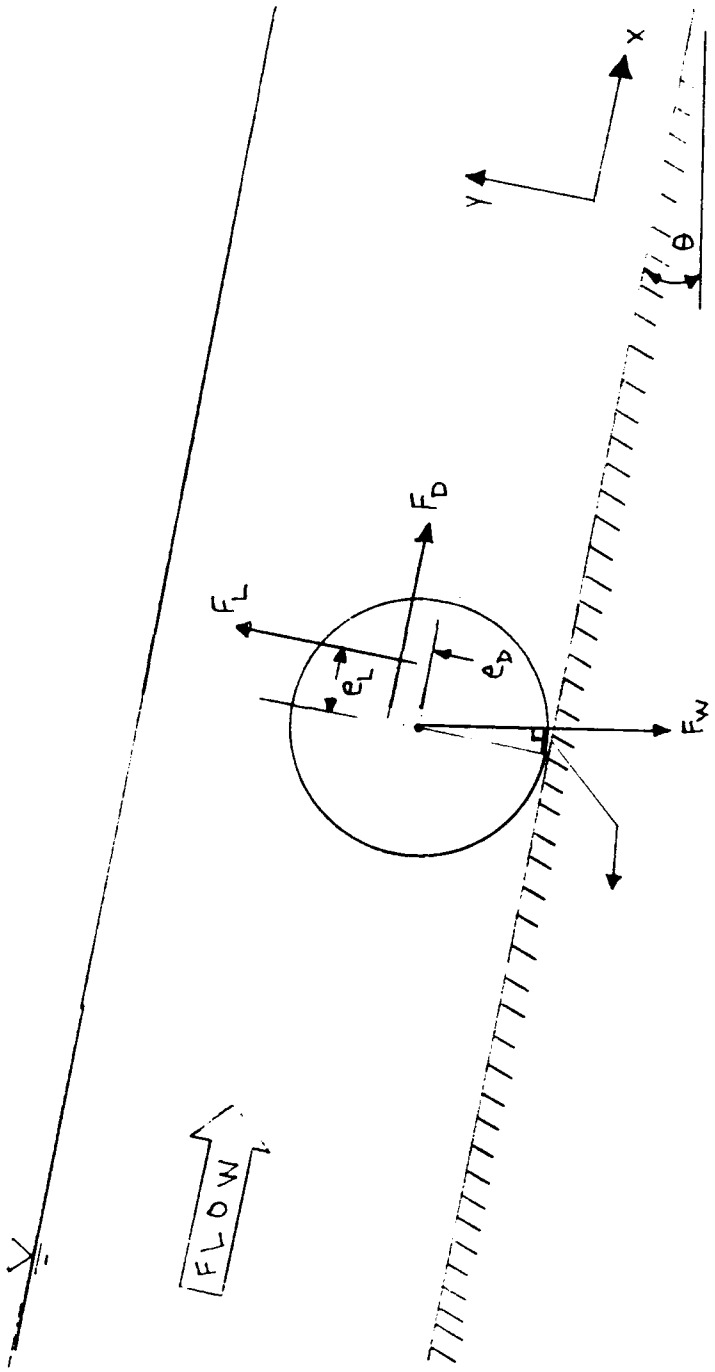

Figure 4.2 Forces on a Submerged Particle for the Case of Rotation

critical velocity, U_{cr}, is a function of $\sqrt{d_s}$, or a function of the particle weight to the 1/6 power. This relationship of critical velocity to weight is known as the one-sixth power law of A. Brahms of 1753.

Note that in all cases, the term A_{sn}, the particle surface area in contact with the flow, changes according to the degree of embedment of the particle as shown in Figure 4.3. Therefore, this term alone can account for all degrees of embedment.

4.1.2 Steady Nonuniform Flow

Figure 4.4 depicts a single particle submerged in a steady nonuniform flow. Incipient motion is conditioned in the same manner as stated for the uniform case. However, the particle is also subject to the force due to the pressure gradient of the nonuniform water surface profile. The equations for drag and lift are rewritten in the following manner

$$Drag = [\int_{A_s} pressure\ dA_s]_{x\text{-}component} + [\int_{A_s} shear\ dA_s]_{x\text{-}component} \qquad (4.14a)$$

$$Lift = [\int_{A_s} pressure\ dA_s]_{y\text{-}component} + [\int_{A_s} shear\ dA_s]_{y\text{-}component} \qquad (4.14b)$$

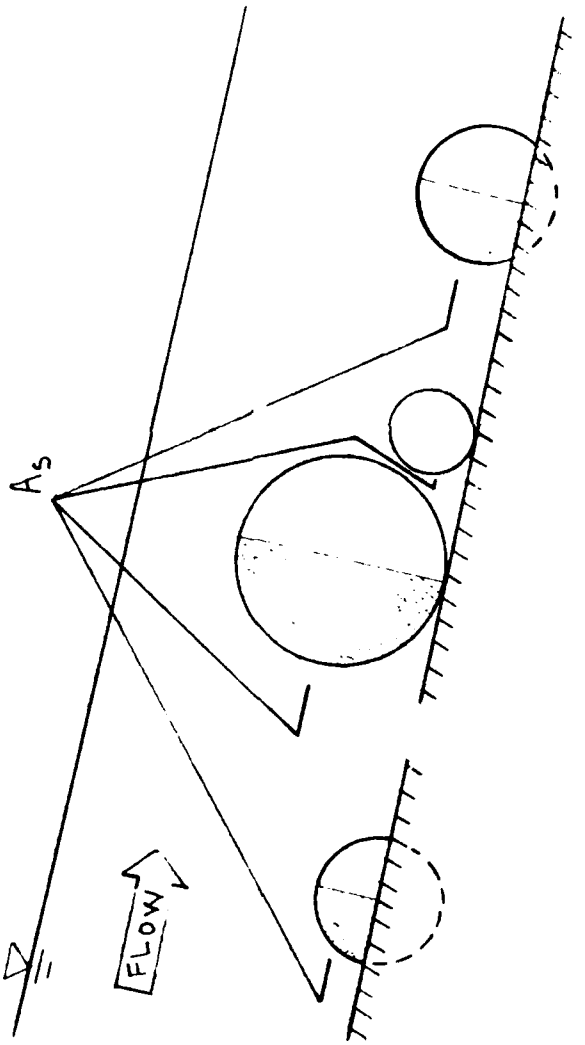

Figure 4.3 Definition Sketch of Particle Embedment

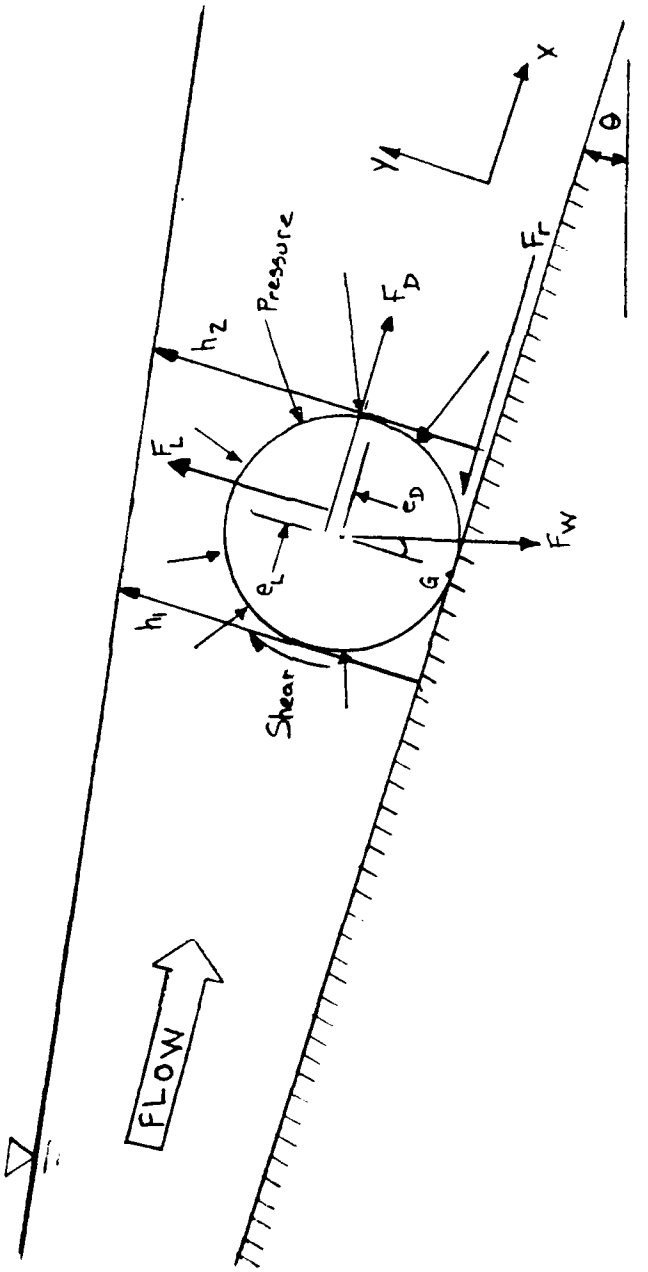

Figure 4.4 Forces on a Submerged Particle in Steady, Nonuniform Flow

The first integral represent the pressure drag and the second term represents the shear drag. The equation for rotation is modified similarly. Therefore, for flow of small or moderate nonuniformity, the critical flow velocity can be written as

$$U_{cr}=K(\beta_s, Re, \frac{dh}{dx})\sqrt{d_s} \qquad (4.15)$$

As stated by Graf (1984, p 37):

> ".... Investigations have shown that there does exist an intricate relationship between the inertia and viscous forces, and only under certain conditions does the problem lend itself to mathematical theory...."

Therefore, most of the complications of the viscous effects are summarized in the drag and lift coefficients C_D and C_L, which are determined by experiment with the same Reynolds number in the laboratory flume as that prevailing in the field. However, most C_D or C_L vs. Re relationships for spheres are for non-rotating, smooth particles surrounded in a fluid with constant approaching velocity.

4.2 THE MOMENTUM APPROACH

The principles of continuity and momentum can be applied to the control volume indicated in Figure 4.5 to obtain a sediment transport equation. Considering the fluid and sediment as two separate control volumes will produce four equations; both a continuity and momentum equation for the sediment and fluid volumes. The continuity equation for the steady flow without lateral flow is

$$U\frac{dA}{dx}+A\frac{dU}{dx}=0 \qquad (4.16)$$

The momentum equation for the fluid is given as Eq. 2.12

$$\frac{dh}{dx}=\frac{S_0-S_f}{1-\frac{\beta U^2}{gD}} \qquad (2.12)$$

where D = A/(water surface width) is the hydraulic mean depth.

The friction slope S_f can be estimated using the Weisbach formula $S_f = fU^2/8gR$, or the Manning formula, $S_f = (n^2U^2)/(2.22\ R^{4/3})$. For unit width, the cross-sectional area, A, is equal to the depth, h. Also, in steady uniform flow, dh/dx = 0, and hence the flow surface slope is equal to the friction slope.

4.2.1 Sediment Equations

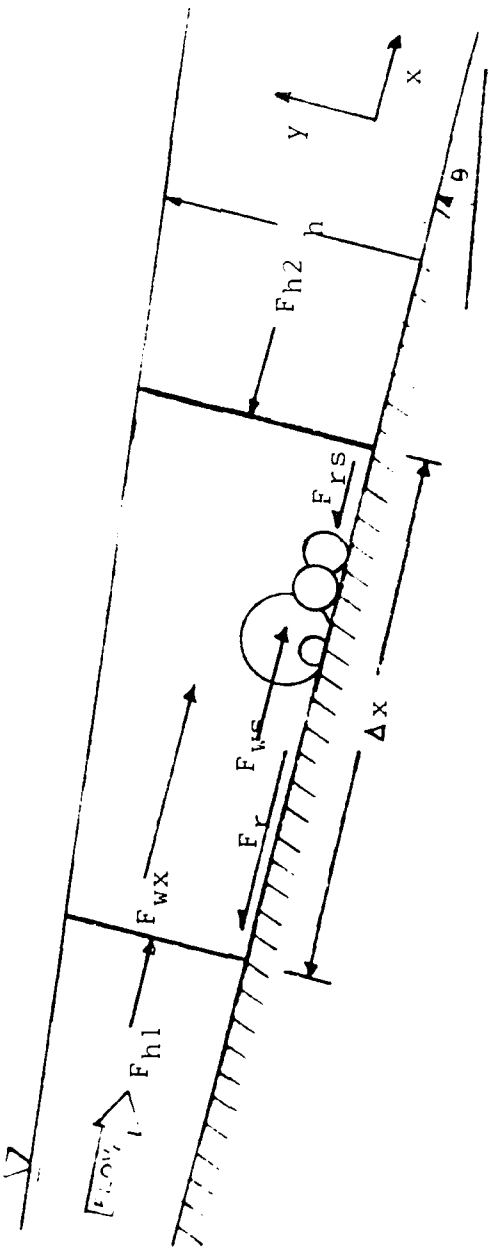

Figure 4.5 Control Volume Sketch of Nonuniform Flow

Assuming a sparse concentration of sediment in the flow on the channel bed, the continuity equation for the sediment is given as

$$q_{s2}=q_{s1}+\frac{\partial q_s}{\partial x}\Delta x \qquad (4.17)$$

where q_s = the sediment discharge per unit width of channel in volume.

At the upstream end of the overland surface, $q_{s1} = 0$. As will be shown later, the sediment volume flux within the control volume is

$$\frac{\partial q_s}{\partial x}=n\xi V_s \qquad (4.18)$$

where n = the number of sediment particles on the bed in the control volume,

$V_s = K_2 d_s^3$ = the volume of a single particle

ξ = a sediment transport efficiency parameter.

The number of sediment particles is a function of the areal packing, A_p, and the square of the characteristic diameter of the particle, d_s. The areal packing is defined as

$$A_p=\frac{A_s'}{A_b}=\frac{nd_s^2K_1}{d_s^2}=nK_1 \qquad (4.19)$$

where A_s' = the area of the channel bed covered by the sediment particles,

A_b = the area of the channel bed,

K_1 = a function of the particle shape and is equal to $\pi/4$ for spheres.

Substituting Eq. 4.18 into Eq. 4.17 provides

$$q_{s2}=q_{s1}+n\xi K_2 d_s^3 \Delta x \qquad (4.20)$$

The momentum equation for the sediment volume can be expressed as

$$\sum F_{xs}=\frac{dm_s U_s}{dt} \qquad (4.21)$$

where F_{xs} = a force acting on the particles in the x-direction,

m_s is the mass of the sediment particles,

U_s is the velocity of the sediment particles in the x-direction.

Since the acceleration of the particles, dU_s/dt is generally unknown and rather difficult to find, Eq. 4.19 provides no useful help in solving for q_s.

Instead, assuming for the particles collectively the acceleration $\Sigma(dU_s/dt)=0$, the force-momentum relationship for the fluid-sediment mixture of the control volume can be written as

$$\frac{d}{dx}(\rho_s\overline{\beta}_s q_s\overline{U_s^2}+\rho\beta AU^2)=\gamma_s S_0 A_s+\gamma S_0 A-\tau_b P_s-\tau_0(P-P_s) \qquad (4.23)$$

where τ_0 = the bed shear over the wetted perimeter P not covered by the particles,

τ_b is the shear on the particles on the boundary occupying a perimeter P_s.

The bar above β_s and U_s indicates averages over the particles, and the particles velocity can be related to U by $U_s = K_5 U$, where the coefficient K_5 is a function of the flow-

particle momentum correction coefficient β_s.

4.3 DETERMINATION OF VELOCITY DISTRIBUTIONS FOR DIFFERENT MOMENTUM CORRECTION COEFFICIENTS

The purpose of this section is show the relationship between the point and mean velocities of the flow over the flow depth or height. Parabolic, logarithmic, and power velocity distributions shown in Figure 4.6 will be considered.

Although the particle is free to move in a three-dimensional manner, only the two-dimensional case will be considered here. Furthermore, only the movement in the down-channel direction (or x-direction) contributes to the sediment transport rate, q_s.

Three Boussinesq coefficients are considered for the study of sediment transport in shallow flow where the flow depth to sediment size ratio is small. One coefficient, β, represents the correction factor for the entire flow depth, h, and the other two relate to the depth at the particle height, d_s. These coefficients are defined by Eq. 4.7 where the reference velocity of the flow is now defined as the mean velocity at the particle height for β_{s1}, and the mean velocity at the flow depth for β and β_{s2}. Therefore,

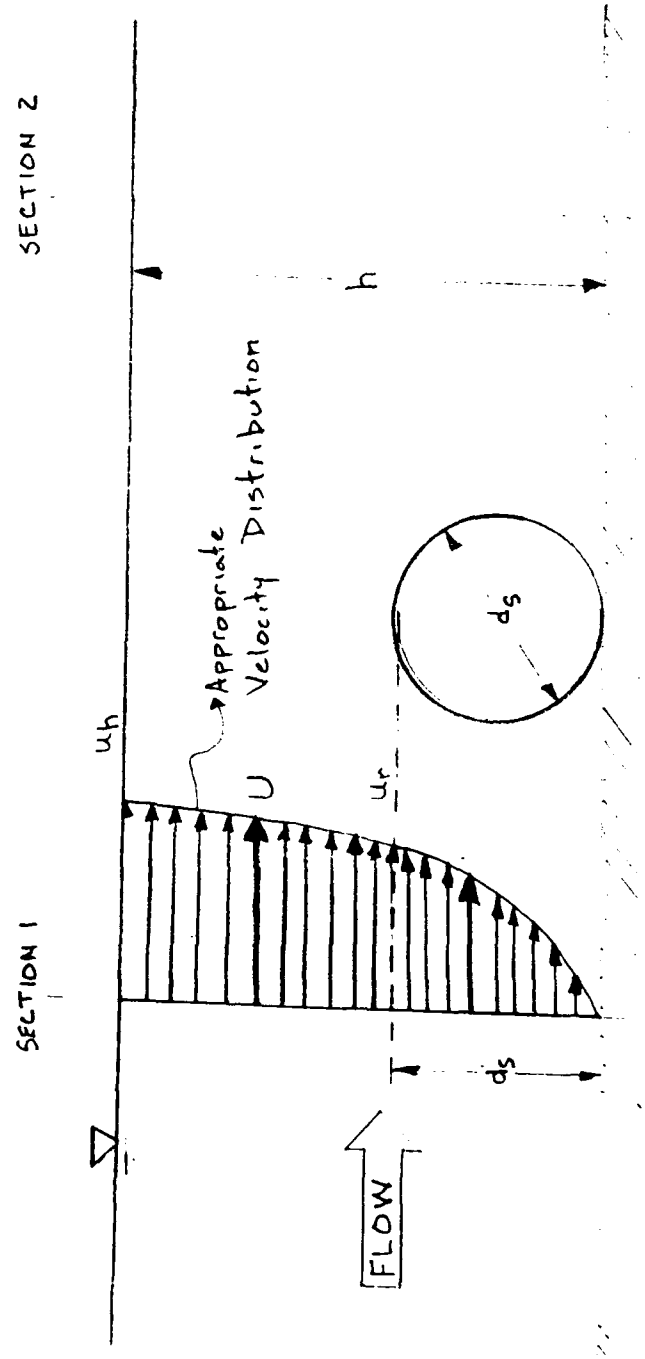

Figure 4.6 Definition Sketch of Velocity Distribution near Particle

$$\beta = \frac{1}{U^2 h} \int_0^h u^2 \, dy \tag{4.24}$$

$$\beta_{s1} = \frac{\int_0^{d_s} u^2 \, dy}{\overline{u_1}^2 d_s} \tag{4.25}$$

$$\beta_{s2} = \frac{\int_0^{d_s} u^2 \, dy}{U^2 h} \tag{4.26}$$

where u = the x component of the local point velocity of the fluid

and u_1 = the average fluid velocity over the particle depth.

$$\overline{u_1} = \frac{1}{d_s} \int_0^{d_s} u \, dy \tag{4.27}$$

A plot of β and β_s versus d_s/h should produce a useful family of curves. For example, as discussed in Section 4.1.1, the incipient motion critical flow velocity is a function of β_s. Since the situation under review concerns a wide channel, β and β_s versus d_s/h represents a unique solution. This would not be the case for a narrow channel where velocity distribution is modified near the surface due to the influence of the walls. Therefore, the three types of velocity distributions mentioned above will be evaluated.

4.3.1 Parabolic Velocity Distribution for Laminar Flow

It is assumed that laminar flow considered here can be represented with a parabolic velocity distribution of the form

$$\frac{u}{u_h} = \left(\frac{2y}{h} - \frac{y^2}{h^2}\right) \tag{4.28}$$

where h = the depth of flow.

The above equation gives the maximum velocity at the water surface, where $u = u_h$. Substituting Eq. 4.28 into Eqs. 4.24, 4.25, and 4.26 and solving provides

$$\beta = \frac{u_h^2}{U^2 h}\int_0^h \left(\frac{4y^2}{h^2} - \frac{4y^3}{h^2} + \frac{y^4}{h^4}\right)\, dy \tag{4.29}$$

Integrating Eq. 4.29 and substituting Eq. 2.17, $U = 2u_h/3$, into it yields

$$\frac{4}{9}u_h^2\beta = \frac{8}{15}u_h^2, \quad \beta = 1.200 \tag{4.30}$$

Similarly, β_{s1} is derived by substituting Eqs. 4.27 and 4.28 into Eq. 4.25 and β_{s2} by Eq. 4.28 into Eq. 4.26. By applying Eq. 2.17 to the result of integration, one has

$$\beta_{s1}=\frac{9}{5}+\frac{3\left(\frac{d_s}{h}\right)-7}{15-10\left(\frac{d_s}{h}\right)+\frac{5}{3}\left(\frac{d_s}{h}\right)^2} \qquad (4.31)$$

$$\beta_{s2}=3\left(\frac{d_s}{h}\right)^3-\frac{9}{4}\left(\frac{d_s}{h}\right)^4+\frac{9}{20}\left(\frac{d_s}{h}\right)^5 \qquad (4.32)$$

Figure 4.7 is a graph of β_{s1} and β_{s2} versus d_s/h for the parabolic velocity distribution.

4.3.2 Logarithmic Velocity Distribution for Turbulent Flow over both Smooth and Rough Boundaries

The turbulent flow velocity distribution has been discussed in Section 2.2.3.2. For a logarithmic velocity distribution over a smooth boundary shown in Figure 2.1,

$$\frac{u}{u_*}=y_* \qquad 0\le y_*\le\delta_* \qquad (4.33)$$

$$\frac{u}{u_*}=5.75\log y_* + 5.5 \qquad \delta_*\le y_*\le h \qquad (4.34)$$

where $y_* = yu_*/\nu$ and $\delta_* = \delta u_*/\nu$

δ = the nominal thickness of the viscous sublayer and is assumed equal to 11.6 for the smooth boundary.

For turbulent flow over a rough boundary, Eq. 4.33 is assumed to still be valid if not obstructed by the roughness element and approximately for $\delta_* \le y_* \le h$

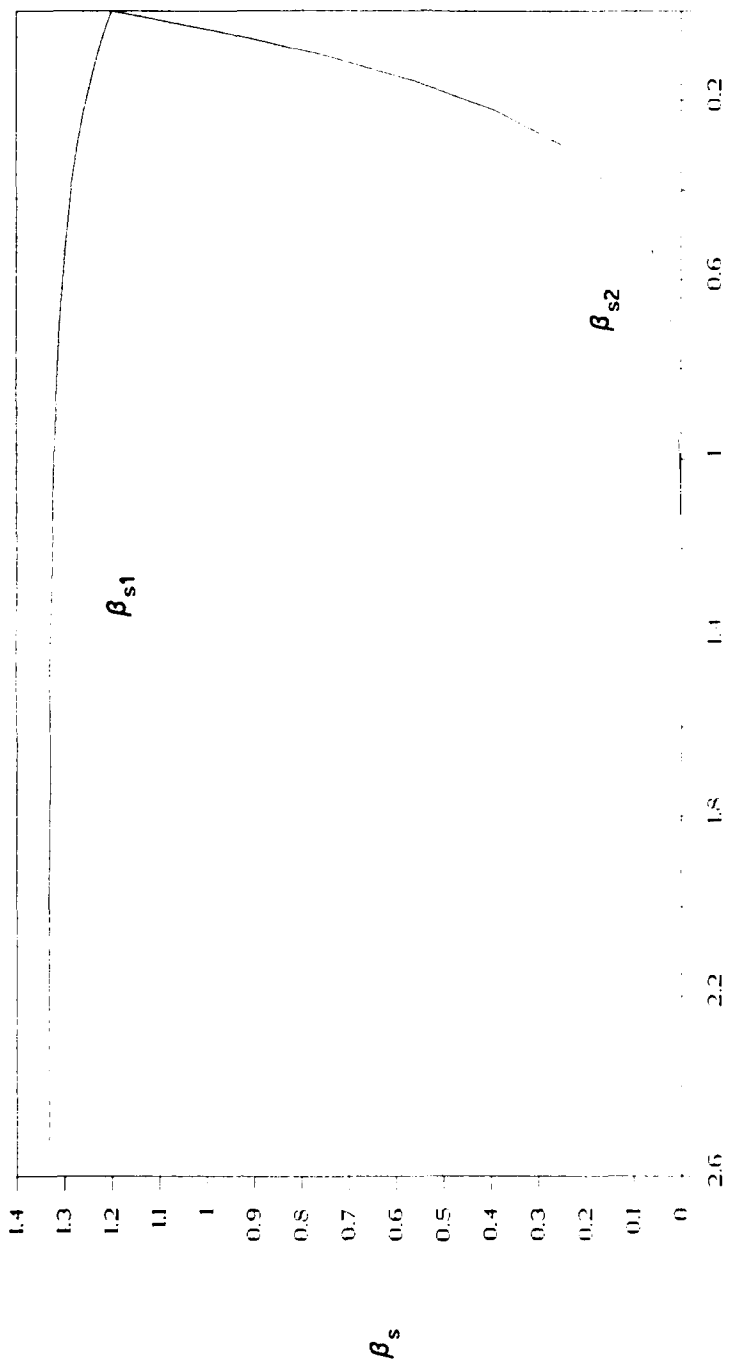

Figure 4.7 β_s vs. d_s/h for Parabolic Velocity Distribution

$$\frac{u}{u_*}=5.75 \log y_* -5.75 \log k_*+ 8.5 \qquad (4.35)$$

where $k_* = (k\, u_*/\nu)$ where k is the roughness height. For the rough boundary case δ_* may be approximated as the intersection of Eqs. 4.33 and 4.35 which implies δ_* being a function of k_*. Accordingly, it has been found that δ_* ranges from 2.49 to 11.6 for which k_* ranges from 27.63 to 3.35.

Substituting Eqs. 4.33 and 4.34 into Eq. 4.24 provides

$$\beta=\frac{1}{U^2 h}\left[\int_0^{\delta_*} y_*^2 dy_* = \int_{\delta_*}^{d_{s*}} (5.75 \log y_* +5.5)^2\, dy_*\right] \qquad (4.36)$$

Integrating Eq. 4.36

$$\beta=1+\frac{(33.06 \log h_* +17.26)^2-\frac{517.59}{h_*}+5.95}{\left(\frac{U_{(\delta)}}{u_*}\right)^2} \qquad (4.37)$$

where

$$\frac{U_{(\delta)}}{u_*}=5.75 \log h_* +3.003-\frac{\delta_*}{h_*}\left(\log \delta_* -3.003-\frac{\delta_*}{2}\right) \qquad (4.38)$$

Similarly, substituting Eq. 4.33 and 4.34 into Eq. 4.25 and 4.26, respectively, and integrating provides

$$\beta_{s1}=1+\frac{(32.06\ \log d_{s*}+17.26)^2-\frac{517.59}{h_*}+5.95}{(\frac{U_{d_s(\delta)}}{u_*})^2} \qquad (4.39)$$

$$\beta_{s2}=1+\frac{d_s}{h}\frac{(32.06\ \log d_{s*}+17.26)^2-\frac{517.59}{d_{s*}}+5.95}{(\frac{U_{(\delta)}}{u_*})^2} \qquad (4.40)$$

where

$$\frac{U_{d_s(\delta)}}{u_*}=5.75\ \log d_{s*}+3.003-\frac{\delta_*}{h_*}(\log \delta_*+3.003-\frac{\delta_*}{2}) \qquad (4.41)$$

For $\delta_* = 11.6$, Eqs. 4.37, 4.39, and 4.40 become

$$\beta=1+\frac{(32.06\ \log h_*+17.26)^2-\frac{517.59}{h_*}+5.95}{(\frac{U_s}{u_*})^2} \qquad (4.42)$$

$$\beta_{s1}=1+\frac{(32.06\ \log d_{s*}+17.26)^2-\frac{517.59}{d_{s*}}+5.95}{(\frac{U_{d_s}}{u_*})^2} \qquad (4.43)$$

$$\beta_{s2}=1+\frac{d_s}{h}\frac{(32.06\ \log d_{s*}+17.26)^2-\frac{517.59}{d_{s*}}+5.95}{(\frac{U_s}{u_*})^2} \qquad (4.44)$$

where

$$\frac{U_s}{u_*}=5.75 \log h_*+3.003-\frac{38.55}{h_*} \qquad (4.45)$$

$$\frac{U_{d_s}}{u_*}=5.75 \log d_{s*}+3.003-\frac{38.55}{d_{s*}} \qquad (4.46)$$

In order to express Eqs. 4.39 and 4.40 in terms of d_s/h, the following equations are substituted

$$d_{s*}=\frac{d_s}{h}h_* \qquad (4.47)$$

$$\log d_{s*}=\log \left(\frac{d_s}{h}\right)+\log h_* \qquad (4.48)$$

$$\log d_s=\log\left(\frac{d_s}{h}\right)\left(\frac{h_*}{k_*}\right) \qquad (4.49)$$

$$\log d_{s*}k_*=\log \left(\frac{d_s}{h}\right)k_*h_* \qquad (4.50)$$

Therefore, using Eqs. 4.47 and 4.48, β_{s1} and β_{s2} can be expressed as

$$\beta_{s1}=1+\frac{[32.1(\log\frac{d_s}{h}+\log h_*)^2+17.3]^2-\frac{517.6}{h_*}(\frac{h}{d_s})+5.95}{(\frac{U_{d_s}}{u_*})^2} \quad (4.51)$$

$$\beta_{s2}=1+\frac{[32.1(\log\frac{d_s}{h}+\log h_*)^2+17.26]^2-\frac{517.6}{h_*}\frac{h}{d_s}+5.95}{(\frac{U_s}{u_*})^2} \quad (4.52)$$

For the rough boundary case, Eqs. 4.33 and 4.35 are substituted into Eq. 4.24

$$\beta=\frac{1}{U^2h}\left[\int_0^{\delta_*} y_*^2 dy_* + \int_{\delta_*}^{d_{s*}} (5.75(\log y_* - \log k_*)+8.5)^2 dy_*\right] \quad (4.53)$$

Integrating Eq. 4.53

$$\beta=1+\frac{B-\frac{\delta_*}{h_*}B-\frac{\delta_*^3}{3}}{(\frac{U_R}{u_*})^2} \quad (4.54)$$

where

$$\frac{U_R}{u_*}=\log\ \frac{h_*}{k_*}+1.04-\frac{\delta_*}{h_*}\left(\log\ \frac{h_*}{k_*}+1.04-\frac{\delta_*}{2}\right) \qquad (4.55)$$

$$B=(5.66\ \log\frac{h_*}{k_*}+8.5)^2-28.72\ \log(h_*k_*) \qquad (4.56)$$

Similarly, substituting Eq. 4.33 and 4.35 into Eq. 4.25 and 4.26, respectively, integrating, and then substituting in Eqs. 4.49 and 4.50 provides

$$\beta_{s1}=1+\frac{B'-\frac{\delta_*}{h_*}\left(\frac{h}{d_s}\right)B'-\frac{\delta_*^3}{3}}{\left[\log\frac{d_s}{h}\frac{h_*}{k_*}+1.04-\frac{\delta_*}{h_*}\frac{h}{d_s}\left(\log\frac{d_s}{h}\frac{h_*}{k_*}+1.04-\frac{\delta_*}{2}\right)\right]^2} \qquad (4.57)$$

$$\beta_{s2}=1+\frac{d_s}{h}\frac{\left(B'-\frac{\delta_*}{h_*}\left(\frac{h}{d_s}B'-\frac{\delta_*^3}{3}\right)\right.}{\left(\frac{U_R}{u_*}\right)^2} \qquad (4.58)$$

where

$$B'=(5.66\ \log\frac{d_s}{h}\frac{h_*}{k_*}+8.5)^2-28.72\ \log\left(\frac{d_s}{h}h_*k_*\right) \qquad (4.59)$$

Graphs of β, β_{s1}, and β_{s2} versus d_s/h are included as Figures 4.8 - 4.12.

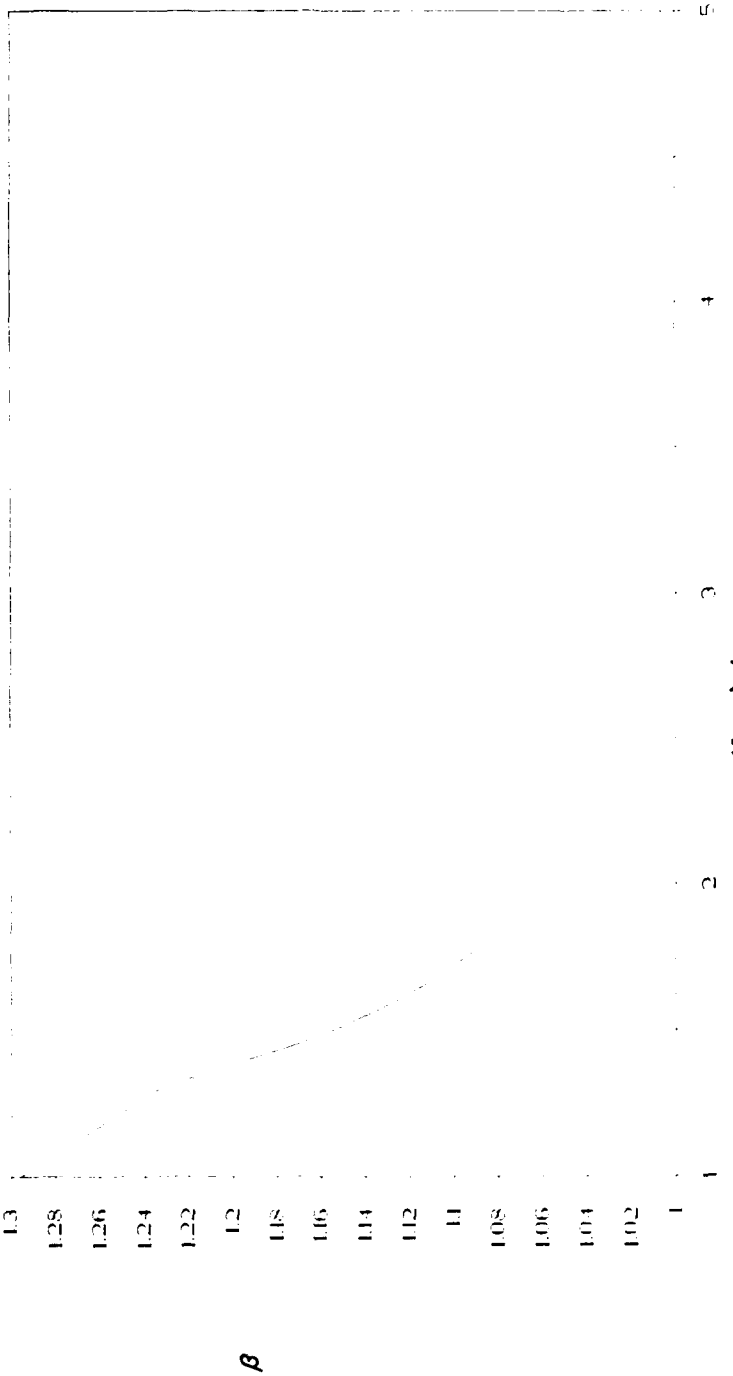

Figure 4.8 Variation of β for Logarithmic Velocity Distribution over a Smooth Boundary

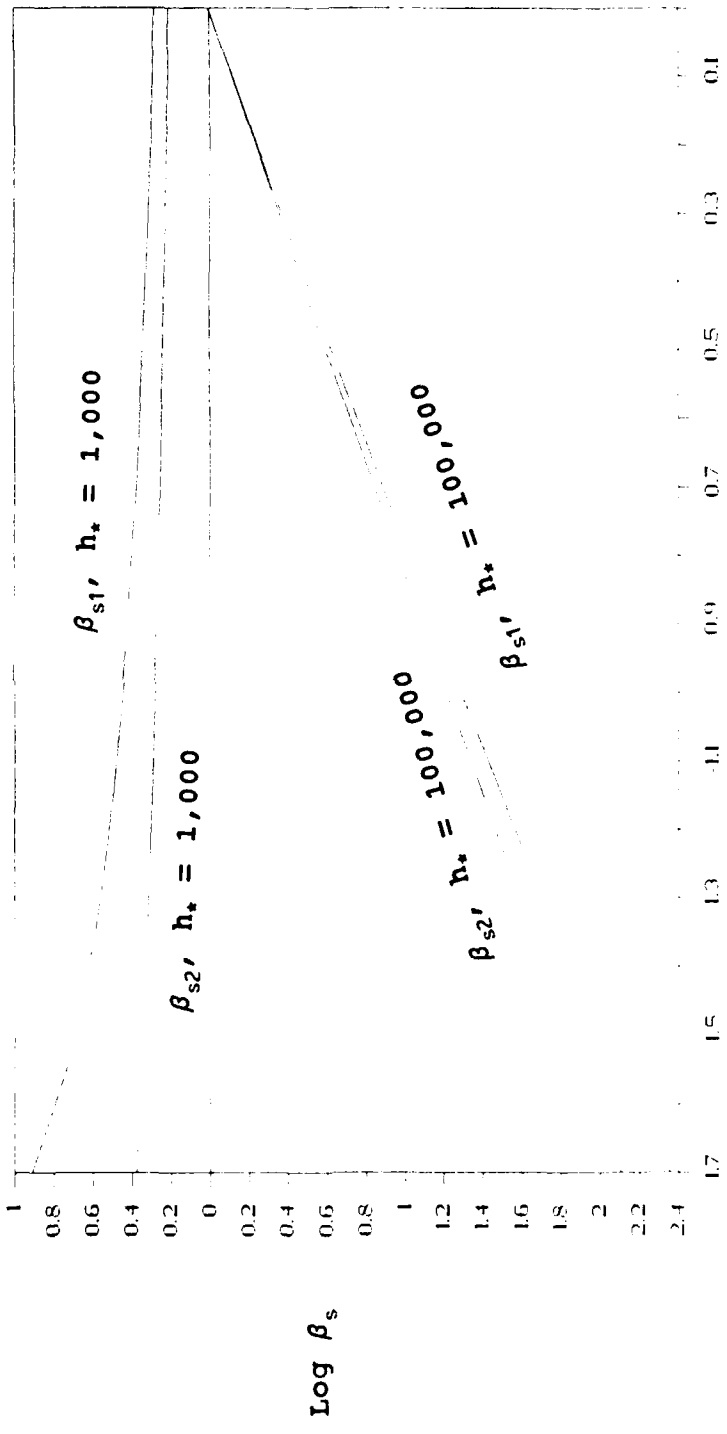

Figure 4.9 Variation of β_s vs. d_s/h for Logarithmic Velocity Distribution over a Smooth Boundary

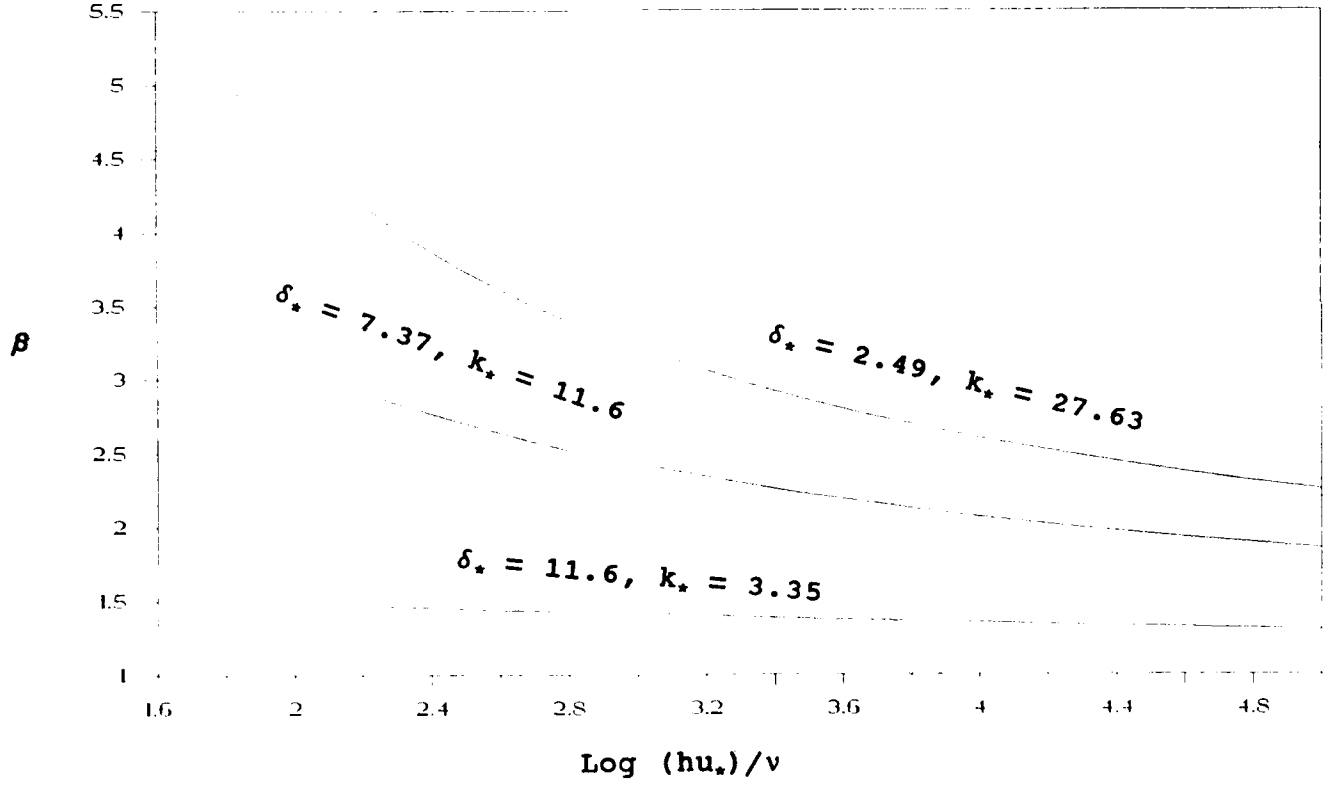

Figure 4.10 Variation of β for Logarithmic Velocity Distribution over a Rough Boundary

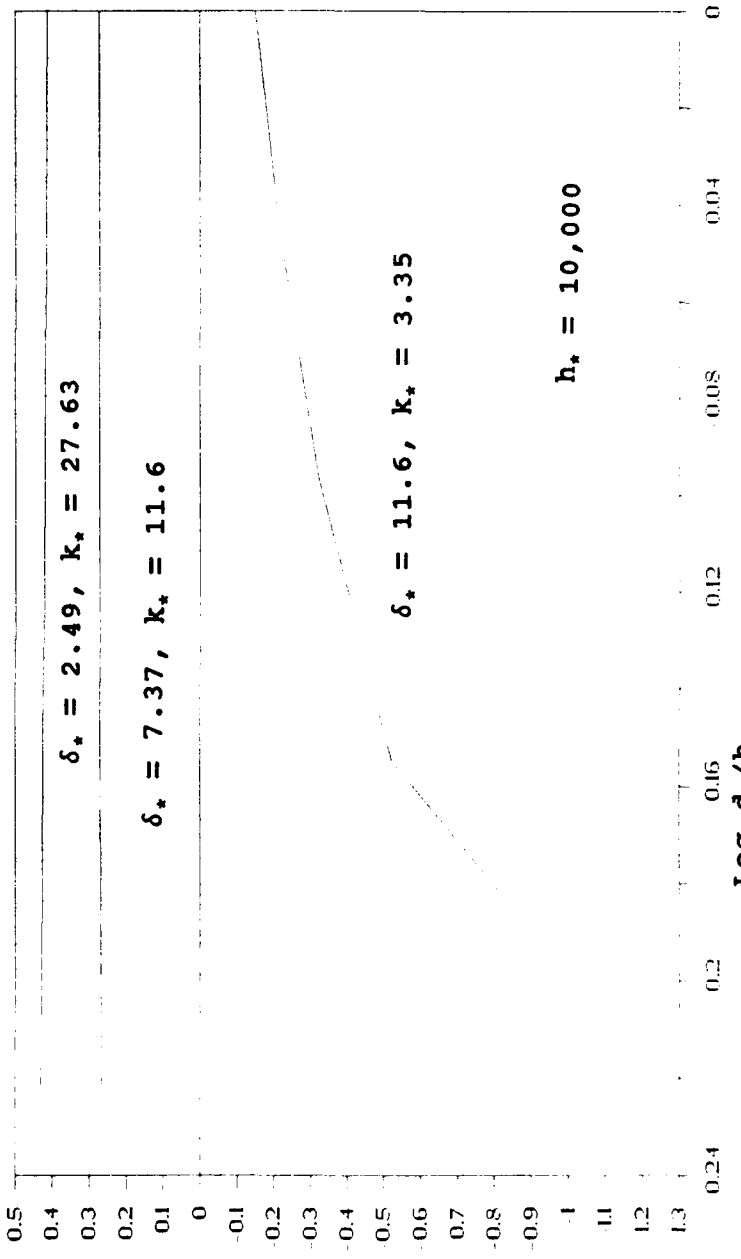

Figure 4.11 Variation of β_{s1} vs. d_s/h for Logarithmic Velocity Distribution over a Rough Boundary

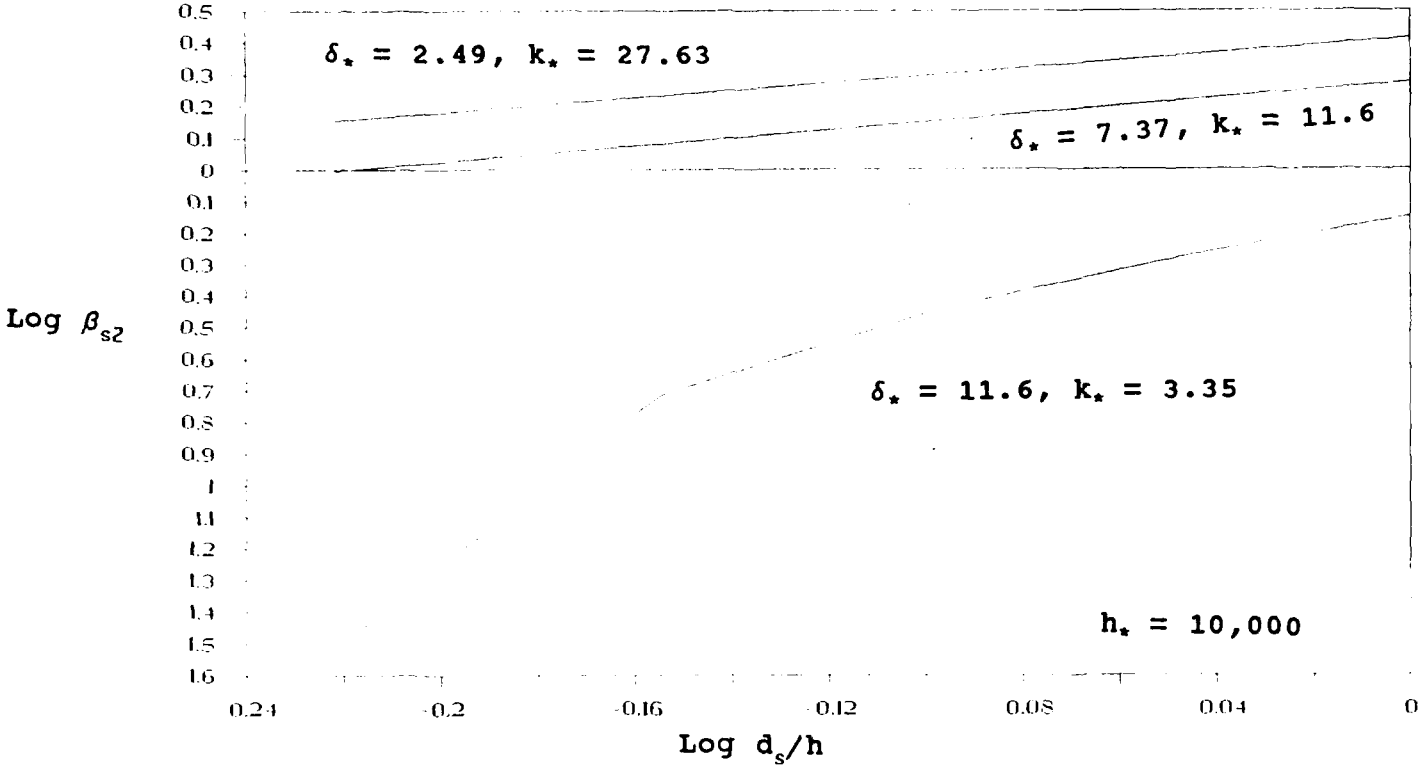

Figure 4.12 Variation of β_s vs. d_s/h for Logarithmic Velocity Distribution over a Rough Boundary

4.3.3 Power Velocity Distribution for Turbulent Flow

Another distribution considered acceptable to represent a turbulent velocity distribution is a power relationship such as

$$\frac{u}{u_h} = \left(\frac{y}{h}\right)^{\frac{1}{m}} \tag{4.60}$$

As before, the equation is evaluated and the following equations are revealed

$$U = \frac{m}{m+1} u_h \tag{4.61}$$

$$\beta = \frac{(m+1)^2}{m(m+2)} \tag{4.62}$$

$$\beta_{s1} = \frac{(m+1)^2}{m(m+2)} = \beta \tag{4.63}$$

$$\beta_{s2} = \frac{(m+1)^2}{m(m+2)} \left(\frac{d_s}{h}\right)^{\left(1+\frac{2}{m}\right)} = \beta \left(\frac{d_s}{h}\right)^{\left(1+\frac{2}{m}\right)} \tag{4.64}$$

$$for\ m=7, \quad \beta = = \beta_{s1} = 1.0208 \tag{4.65}$$

$$\beta_{s2} = 1.0208 \left(\frac{d_s}{h}\right)^{\frac{8}{6}} \tag{4.66}$$

$$for\ m=7,\quad \beta==\beta_{s1}=1.0159 \tag{4.67}$$

$$\beta_{s2}=1.0159\left(\frac{d_s}{h}\right)^{9/7} \tag{4.68}$$

A graph of β, β_{s1}, and β_{s2} for m=6 and m=7 is given in Figure 4.13.

As can be seen in the various graphs, β_{s2} is not particularly useful in this study. Originally, β_{s2} was developed in order to possibly combine the effect of β and β_{s1}, and therefore eliminate one variable. However, both β and β_{s1} must be used.

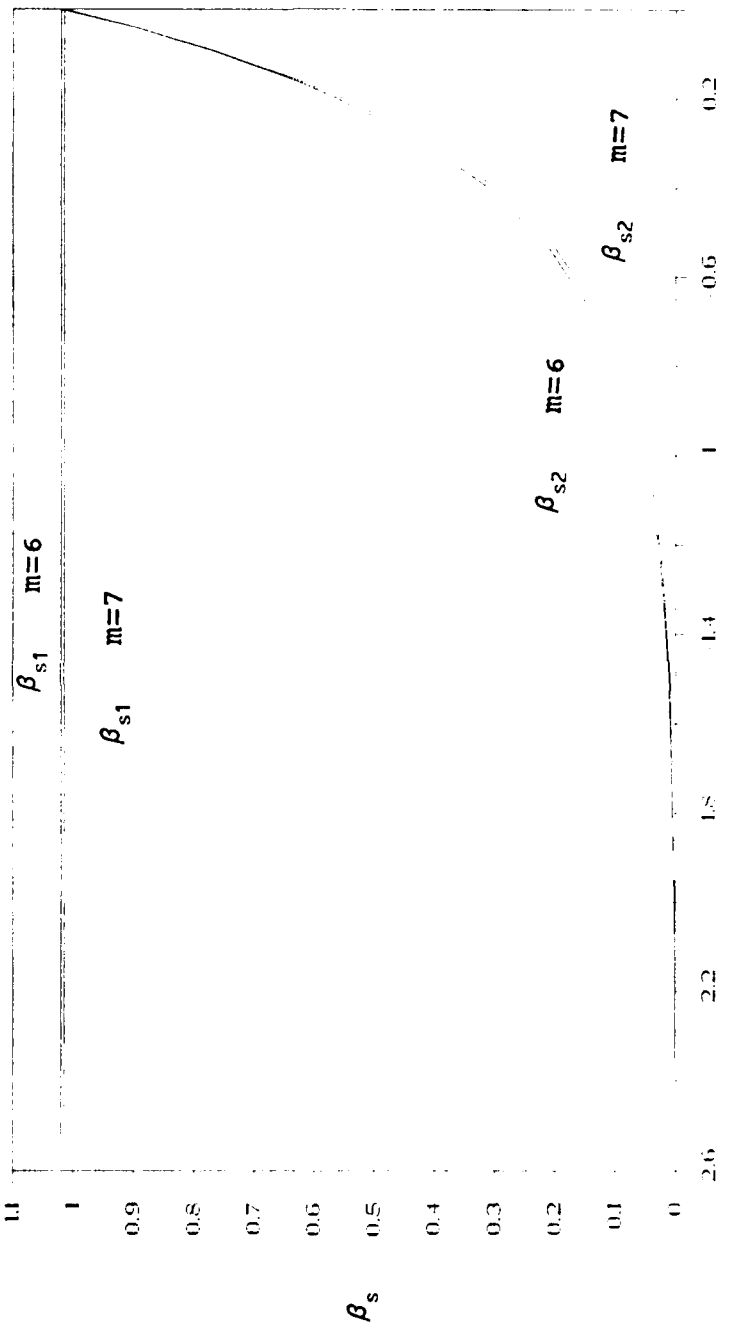

Figure 4.13 Variation of β_s vs. d_s/h for Power Velocity Distribution

5. DEVELOPMENT OF THE MODEL

After identification of the variables affecting sediment transport, the use of dimensional analysis has indicated which dimensionless combinations of these parameters are most significant. Theory has identified the forces acting on a single submerged particle and the use of the momentum equation has provided an equation for sediment transport which could be calibrated and verified given sufficient data. The momentum flux correction coefficients for both the total flow depth and that associated particle depth have been found in equation form and are presented in graphs. The employment of these correction coefficients allows velocity distribution to be represented in the final sediment transport equation. Therefore, given the above information, a model is developed for sediment transport in shallow flow on an impervious surface. Data is not presently available for this particular case so assumptions are required that when the data is obtained, the chosen parameters can be found. However, in order to verify the work of this thesis, some existing sediment transport work is employed in a modified manner.

The sediment transport model is developed by defining an incipient motion parameter to predict particle movement and an efficiency parameter to predict the portion of particles set into motion which actually are transported

from the reach of the channel under consideration.

5.1 INCIPIENT MOTION PARAMETER

As described previously, incipient motion occurs when the forces acting to move the submerged particle are equal to those preventing movement. Because of the complexity and nature of the movement of a particle within the flow, incipient motion is often used as an indicator of the transport. The complexities involved in the study of sediment transport prevents the determination of the parameter from theory by using the equations of motion.

Previous studies on the terminal fall velocity of particles of different sizes often provides useful information in the study of sediment transport where the flow depth is much greater then the particle size. However, because of the shallow flow, the particle is always accelerating or decelerating and never reaches its true terminal velocity.

However, it is known that the pickup parameter is a function of the particle size to depth ratio, d_s/h, the Reynolds number of the flow, Re, and the level of turbulence in the flow. In this study, the pickup parameter is defined as when the particles are set into motion and is denoted by Ω. Ω has a value between 0 and 1.

Since not all particles which are set into motion are actually transported out of the reach under consideration, a second parameter is required for the model. This parameter is the deposition parameter, M, and will be related to Ω by an efficiency parameter developed in Section 5.2.

The pickup parameter is approximated by using the Shields diagram. Also, a second means of finding the parameter from known graphs of the drag coefficient, C_D, versus Reynolds number for a sphere is discussed.

5.1.1 Approximation using Shields Diagram

Figure 5.1 provides a modified Shields diagram by Yalin and Karahan (1979) which can be expressed as

$$Y_{cr} = F(X_{cr}) \tag{5.1}$$

where

$$X_{cr} = \frac{u_* d_s}{\nu} \tag{5.2}$$

$$Y_{cr} = \frac{\tau_0}{(\gamma_s - \gamma)\, d_s} \tag{5.2}$$

In addition to the curve representing incipient motion in turbulent flow, Yalin and Karahan have provided a curve for laminar conditions. The laminar line is based on laboratory

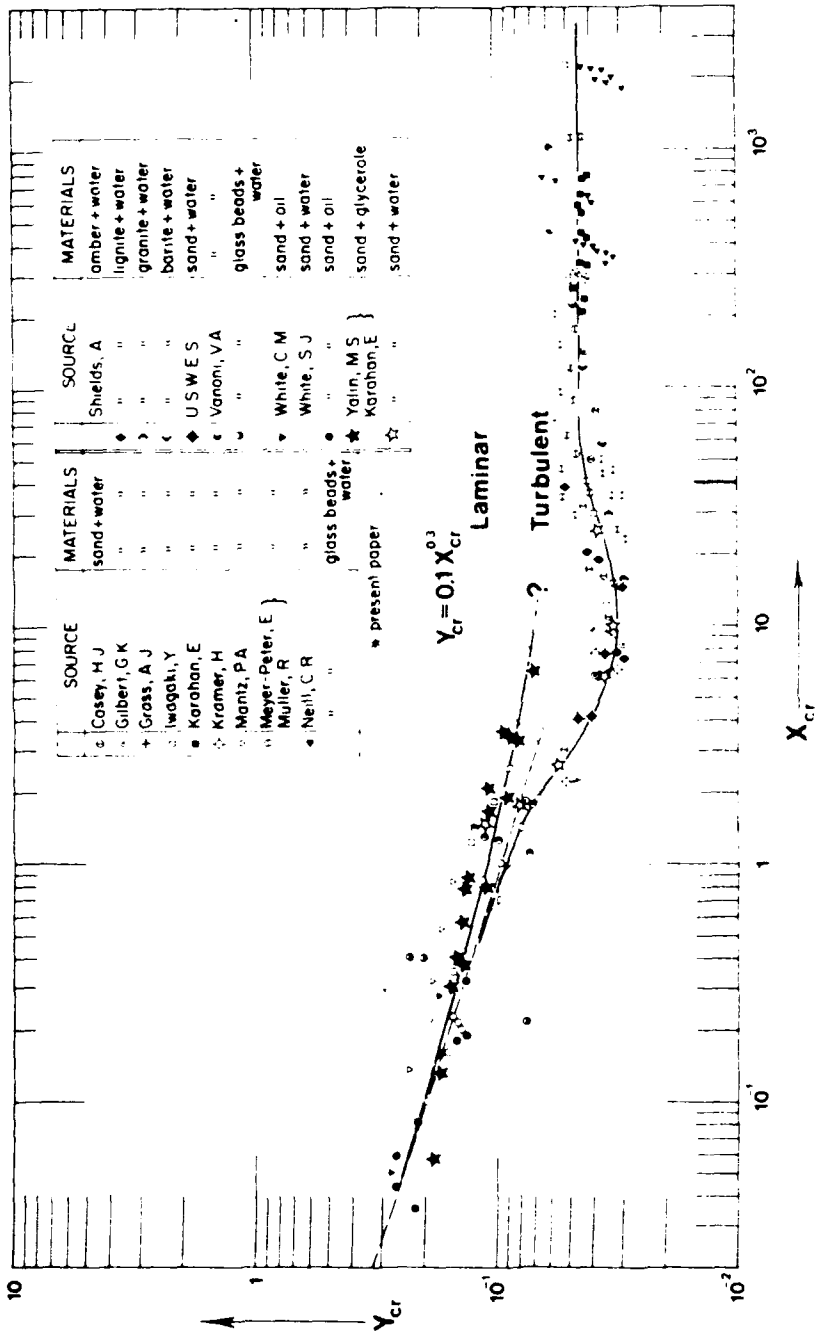

Figure 5.1 Modified Shields Diagram

(from Yalin and Karahan, 1979)

flume data. Therefore, it is considered that the two curves can adequately describe both turbulent and laminar steady uniform flow which is studied in this research.

The procedure for predicting motion given the curves of the modified Shields diagram is to find the value of the dimensionless parameter $U_{cr}/\sqrt{gd_s}$ as a function of the Shields diagram and d_s/h, the bed slope (S_0), and the Reynolds number at which the flow is capable of inducing particle motion, Re_h.

5.1.1.1 Steady Uniform Flow

For a steady uniform flow $\tau_0=\gamma hS_0$, the Shields diagram ordinate becomes

$$\frac{\tau_0}{(\gamma_s-\gamma)\,d_s}=\frac{\gamma hS_0}{(\gamma_s-\gamma)\,d_s}=\left(\frac{\rho}{\rho_s-\rho}\right)\frac{h}{d_s}S_0 \qquad (5.4)$$

Also for steady uniform flow, the abscissa is given as

$$\frac{d_s\sqrt{\frac{\tau_0}{\rho}}}{\nu}=\frac{d_s\sqrt{ghS_0}}{\nu}=\frac{\sqrt{gd_s}}{U_{cr}}\sqrt{\frac{d_s}{h}S_0Re_c} \qquad (5.5)$$

where $Re_c = U_{cr}\,h/\nu$ is the flow Reynolds number at the sediment incipient motion condition.

The Shields diagram (Figure 5.1) provides Eq. 5.4 as a

function of Eq. 5.5. i.e.

$$\frac{\sqrt{gd_s}}{U_{cr}}\sqrt{\frac{d_s}{h}S_0}Re_c=F^{-1}\left[\left(\frac{\rho}{\rho_s-\rho}\right)\frac{h}{d_s}S_0\right] \qquad (5.6)$$

Therefore, the dimensionless critical velocity relationship can be expressed as

$$\frac{U_{cr}}{\sqrt{gd_s}}=\sqrt{\frac{d_s}{h}}Re_c\sqrt{S_0}\quad F\left[\frac{1}{\left(\frac{\rho_s}{\rho}\right)-1}\frac{h}{d_s}S_0\right] \qquad (5.7)$$

or

$$\frac{U_{cr}}{\sqrt{gd_s}}=\frac{d_s}{h}Re_c\sqrt{S_0}\quad F\left[\frac{h}{d_s}\frac{S_0}{\left(\frac{\rho_s}{\rho}\right)-1}\right] \qquad (5.8)$$

For $\rho_s/\rho = 2.65$

$$\frac{U_{cr}}{\sqrt{gh}}=\left(\frac{d_s}{h}\right)Re_c\sqrt{S_0}\quad F\left[\frac{h}{d_s}\frac{S}{1.65}\right] \qquad (5.9)$$

$$also\ \frac{U_{cr}}{\sqrt{gd_s}}=\sqrt{\frac{d_s}{h}}\ Re_c\sqrt{S_0}\quad F\left[\frac{d_s}{h}^{-1}\frac{S_0}{1.65}\right] \qquad (5.10)$$

The difference of the function F for laminar and turbulent flows given in Yalin and Karahan's diagram (Figure 5.1) is due to the difference in velocity distribution as reflected

by the momentum correction coefficient β as indicated by Eq. 3.4 from dimensional analysis. Plots of Eqs. 5.9 and 5.10 on the basis of Yalin and Karahan's diagram are provided as Figures 5.2 and 5.3. Note that the particular curve selected from the Shields diagram is determined by the flow Reynolds number. Chow (1959) suggests a transitional Reynolds number for open channel flow of 500 to 2,000.

5.1.1.2 Steady Nonuniform Flow

As an approximation, the Shields diagram may also be applied to incipient motion in shallow flow in a wide channel assuming the flow is under hydrostatic pressure distribution (Figure 4.4). For a unit width, the pressure difference between one section (1) of the fluid volume to another (2) can be expressed as

$$\Delta p=\frac{1}{2}\gamma(h_2^2-h_1^2)\cos\theta\approx\gamma\cos\theta\,\bar{h}\Delta h \qquad (5.11)$$

The x component of the weight of the fluid, F_{wx}, and the shear force on the boundary, F_τ, of the control volume are expressed as

$$F_{wx}\approx[\frac{\gamma}{2}(h_1+h_2)\Delta x]\sin\theta \qquad (5.12)$$

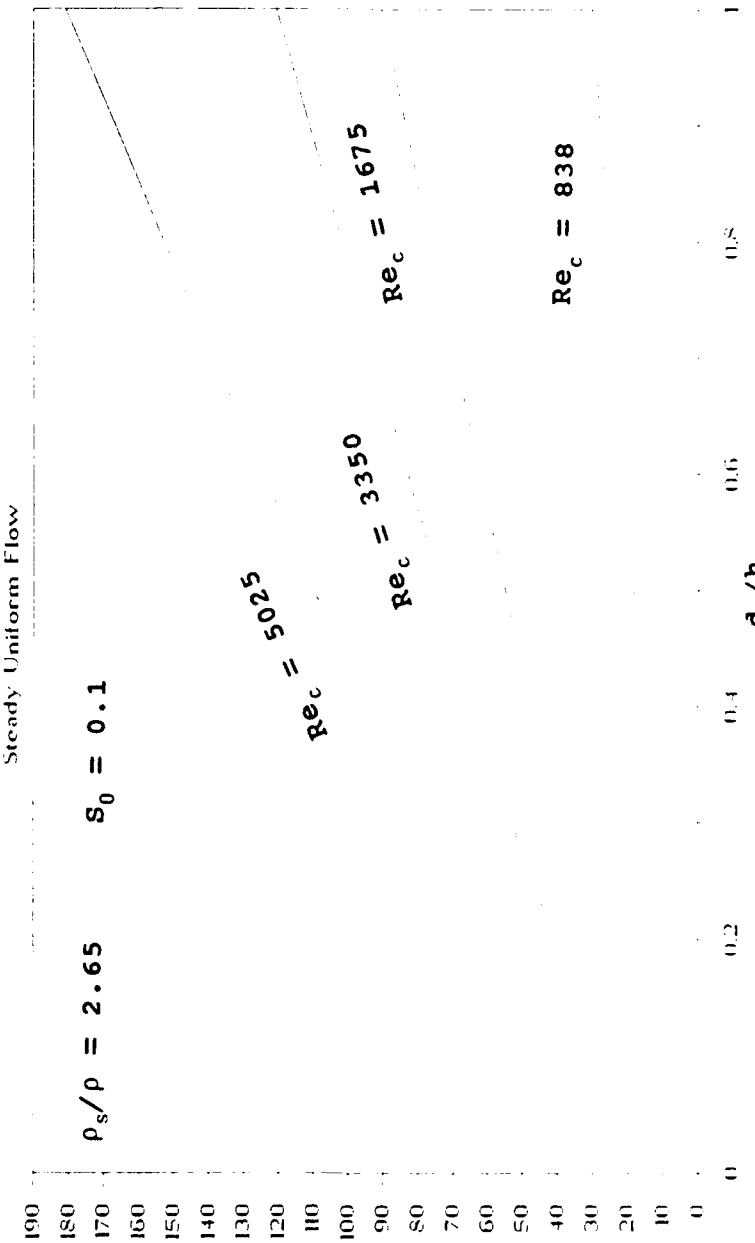

Figure 5.2 Critical Velocity vs. d_s/h for Uniform Flow

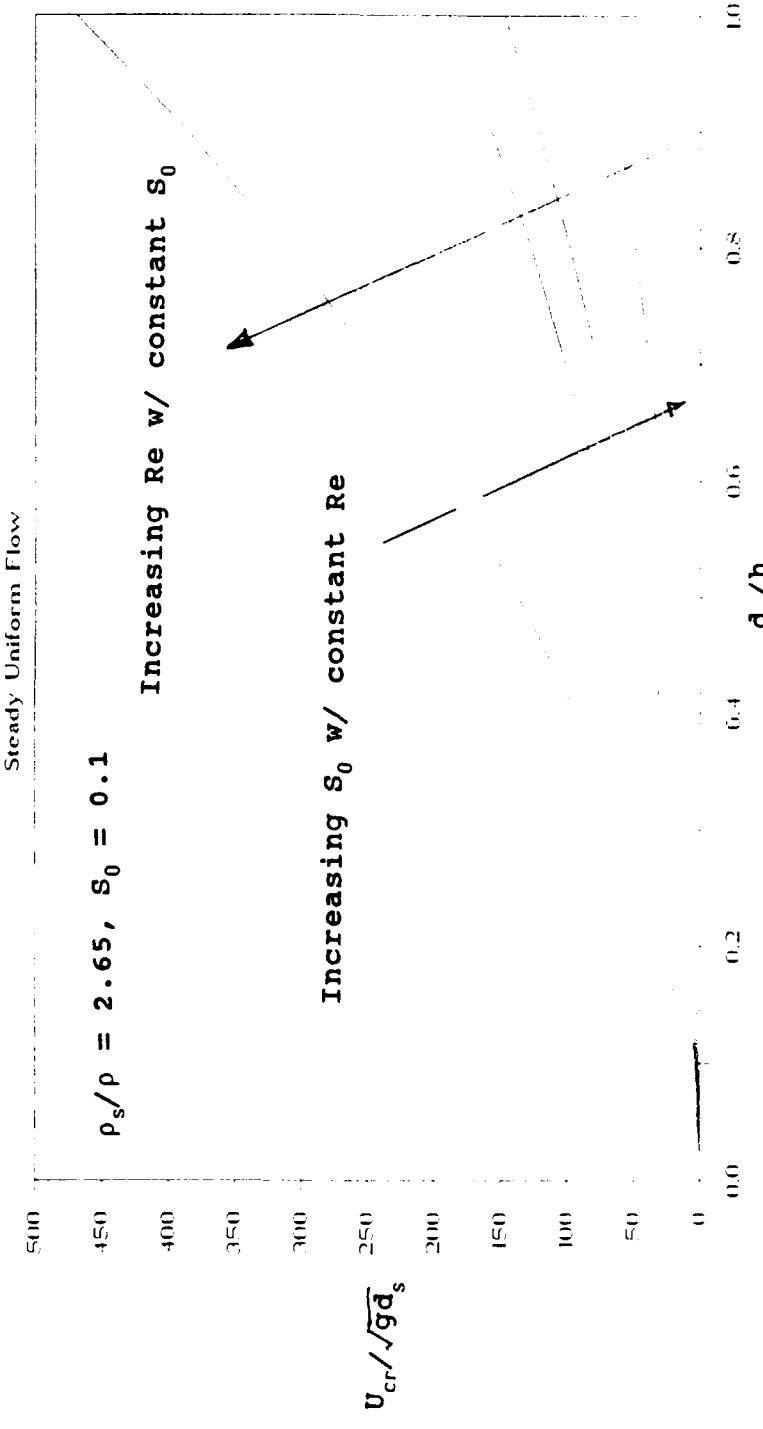

Figure 5.3 Critical Velocity vs. d_s/h for Uniform Flow

$$F_\tau = \tau_0 \Delta x \qquad (5.13)$$

With incipient motion occurring at $\Sigma F_x = F_{wx} - F_\tau - \Delta p = 0$, the following relationship is obtained

$$\tau_0 = \gamma h \sin\theta - \gamma \cos\theta \; h \frac{dh}{dx} \qquad (5.14)$$

Defining $S_f = \tau_0/(\gamma h)$ and noting that $S_0 = \sin\theta$, we have

$$S_f = S_0 - \cos\theta \frac{dh}{dx} \qquad (5.15)$$

Thus, if the effect of $dh/dx \approx S_w$ directly on the sphere is assumed negligible, the steady uniform relationships that were obtained in Section 5.1.1.1 can be used as an approximation provided S_0 is replaced by $S_0 - \cos\theta \; S_w$. Thus, for small θ, from Eq. 5.9, noting that $u_* = \sqrt{ghS_0}$,

$$\frac{U_{cr}}{u_*} \frac{1}{Re_c} = \frac{d_s}{h} F\left[\left(\frac{d_s}{h} \right)^{-1} \frac{S_0 - S_w}{1.65} \right] \qquad (5.16)$$

A graph of this relationship for nonuniform flow is given as Figure 5.4.

5.1.2 Approximation Using Particle Drag and Lift Graphs

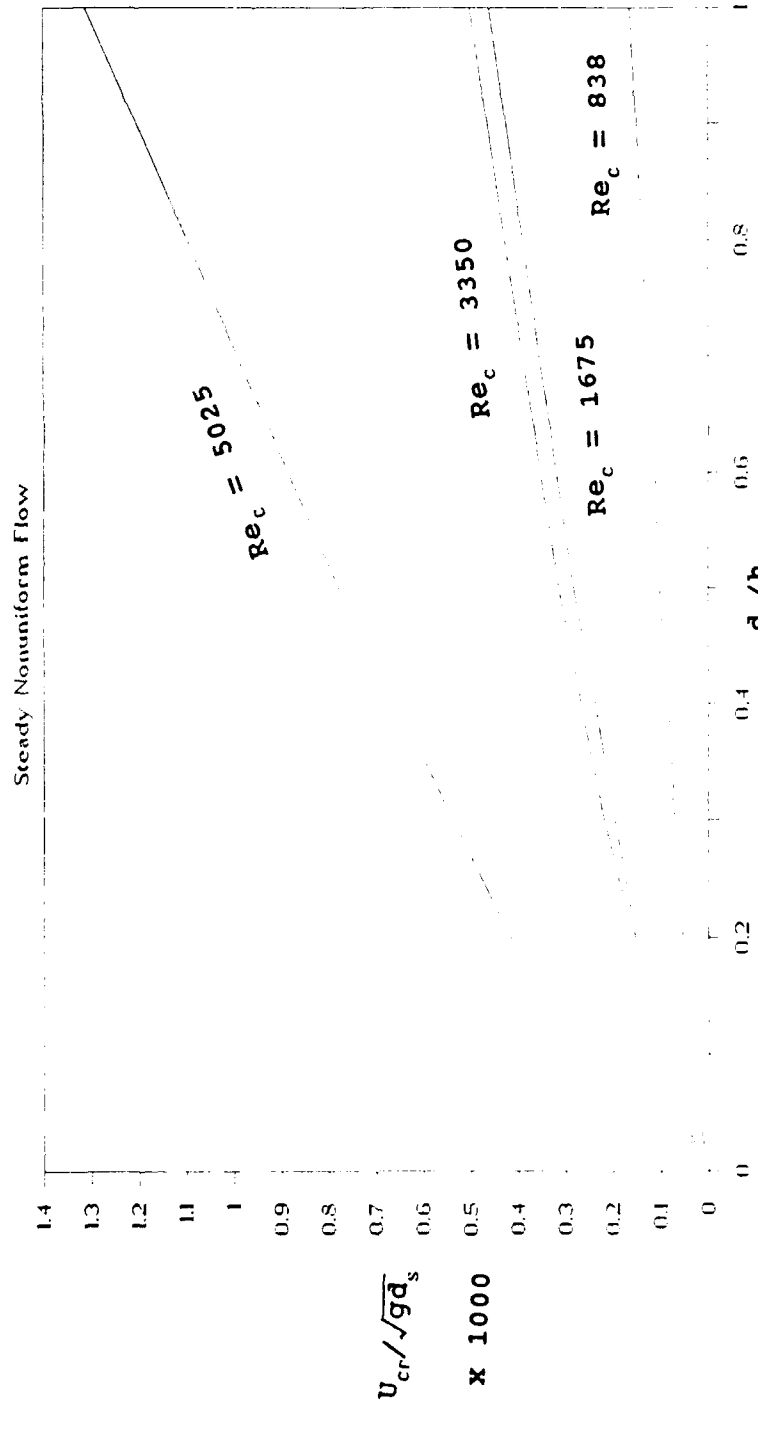

Figure 5.4 Critical Velocity vs. d_s/h for Nonuniform Flow

Incipient motion can be induced by any combination of lift, drag, or rotation as discussed in section 4.1. The case of incipient motion can be expressed as

$$\omega (F_L - F_{wy}) + (1-\omega)(F_D - F_{wx}) = 0^+ \qquad (5.17)$$

where ω = a weighing factor for the relative importance between lift and drag on incipient motion,

F_L is the lift force,

F_D is the drag force,

F_{wx} is the submerged particle weight in the x-direction,

and F_{wy} is the submerged particle weight in the y-direction.

Inserting Eqs. 4.1, 4.2, and 4.3 for the drag, lift, and weight, respectively, into Eq. 5.17 yields

$$\omega \left[C_L \beta_s U_r^2 - \frac{4}{3}\left(\frac{\rho_s}{\rho} - 1\right) g d_s\right] + (1-\omega)\left[C_D \beta_s U_r^2 - \frac{4}{3}\left(\frac{\rho_s}{\rho} - 1\right) g d_s S_0\right] = 0 \qquad (5.18)$$

where S_0 = sin θ,

U_r = reference velocity at the sphere center,

cos θ = 1 for a small θ.

Since it has been shown that U_{cr}/U_r is a function of β and β_s, Eq. 5.16 can be rewritten as

$$\frac{U_{cr}^2}{g d_s} F(\beta, \beta_s)\left[\omega C_L + (1-\omega) C_D\right] = \frac{4}{3}\left(\frac{\rho_s}{\rho} - 1\right)\left[\omega + (1-\omega) S_0\right] \qquad (5.19)$$

where F = a function.

Values of the lift and drag coefficients can be approximated for a sphere from previously published graphs of C_L or C_D versus the flow Reynolds number like the one given as Figure 5.5. Values of ω and $F(\beta,\beta_s)$ are currently unknown. However, these parameters could be found with sufficient experimental data when available. Once ω and $F(\beta,\beta_s)$ are known, U_{cr}^2/gd_s can be calculated since all other variables are known or available. The critical velocity can then be found and compared against the actual mean velocity of the flow to see if the flow is capable of initiating sediment into motion.

5.2 SEDIMENT TRANSPORT EFFICIENCY PARAMETER

It is assumed that once incipient motion occurs, the flow has a unique and specific transport efficiency which is a function of the local conditions. The sediment transport efficiency parameter is denoted by ξ' and it is defined as the fraction of the particles set into motion which are actually transported from the reach under consideration. Since the pickup (Ω) and deposition (M) parameters are functions of the same variables, the two can be related by a new function,

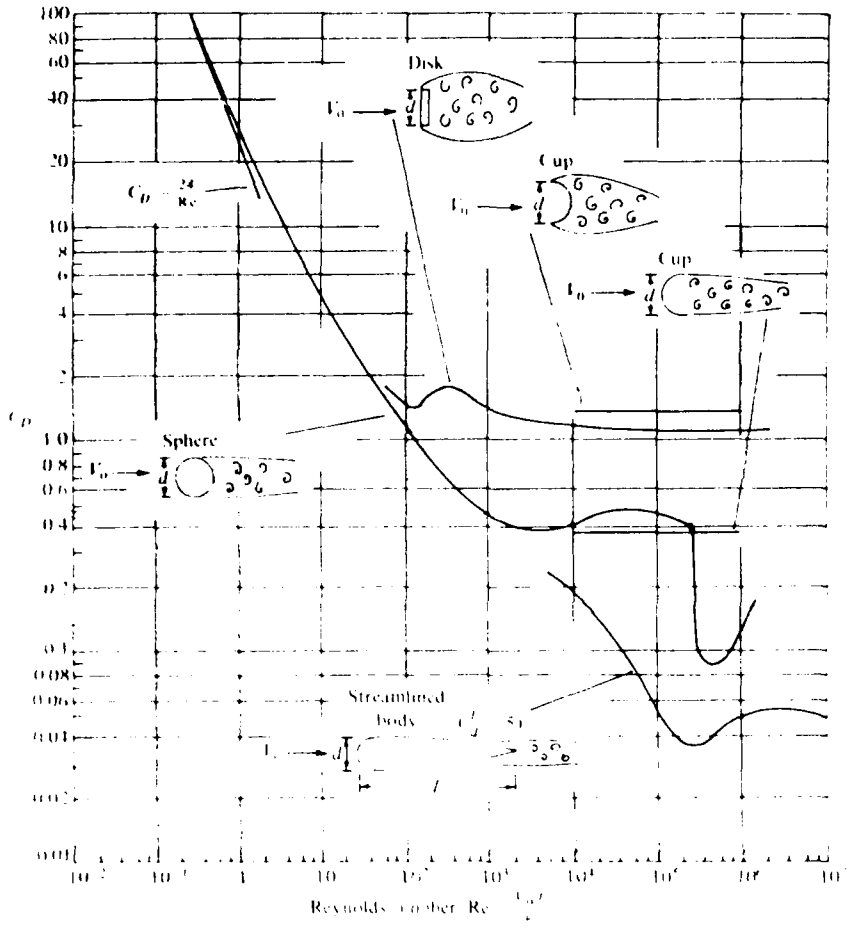

Figure 5.5 Drag Coefficient vs. Reynolds Number for a Particle held in Approaching Flow with Uniform Velocity Distribution Flow (from Robeson and Crowe, 1985)

$$M=K_6\Omega-\frac{K_7}{\Omega} \tag{5.20}$$

when Ω is greater than M, erosion occurs and when the reverse is true, sedimentation occurs. If we let $\xi'=(\Omega-M)$ and substitute this into Eq. 4.18,

$$nV_s(\Omega-M)=\frac{dq_s}{dx} \tag{5.21}$$

where n = the number of particles available for transport within the given reach of unit area.

Therefore, from Eq. 5.22

$$\frac{dq_s}{dx}=nV_s(\Omega-K_6\Omega-\frac{K_7}{\Omega})=nV_s\Omega(1-K_6-\frac{K_7}{\Omega^2}) \tag{5.22}$$

Therefore, $\xi' = (\Omega-M) = K_7\Omega$, ranges from 0 to 1 and would be determined through experimentation. Ω, M, and ξ' all have the units of 1 per time (1//T). The characteristics of ξ' can be determined by examining Ω and M. Ω is a function of U_{cr} as shown by

$$\frac{\Omega h}{U}=F_1(\frac{U_{cr}}{\sqrt{gd_s}},\beta,\frac{\rho_s}{\rho},Re,\frac{d_s}{h},\frac{U}{U_{cr}}) \tag{5.24}$$

Therefore, Ω, M, and ξ' can all be expressed as a function of the critical velocity expressed as $(U-U_{cr})/U_{cr}$. Values for the critical velocity expression is obtained from both

physical theory and past laboratory work. The physical view of drag, lift and rotation on a submerged particle provided Eqs. 4.8, 4.11, and 4.13 where U_{cr} is expressed as a function of a K function and d_s. Eqs. 4.8, 4.11, and 4.13 can be modified by the gravitational acceleration constant, g, to provide

$$Drag: \quad \frac{U_{cr}}{\sqrt{gd_s}} = g\ K_D \tag{5.26}$$

$$Lift: \quad \frac{U_{cr}}{\sqrt{gd_s}} = g\ K_L \tag{5.27}$$

$$Rotation: \quad \frac{U_{cr}}{\sqrt{gd_s}} = g\ K_R \tag{5.28}$$

where K = a function.

The use of Shields diagram provided Eq. 5.10 to find a value for the critical velocity expression.

A suggested plot of Ω and M versus the dimensionless critical velocity expression $(U-U_{cr})/U_{cr}$ is given in Figure 5.6 and 5.7, respectively. Both the ideal and actual cases are given. The actual case differs from the real due to the bursting effect in turbulent flow and the temporal variations of the wake in laminar flow. Since the velocity fluctuates or varies with time, the particle may be set into motion at a particular instant when the flow conditions warrant it even though the average flow has not reached the

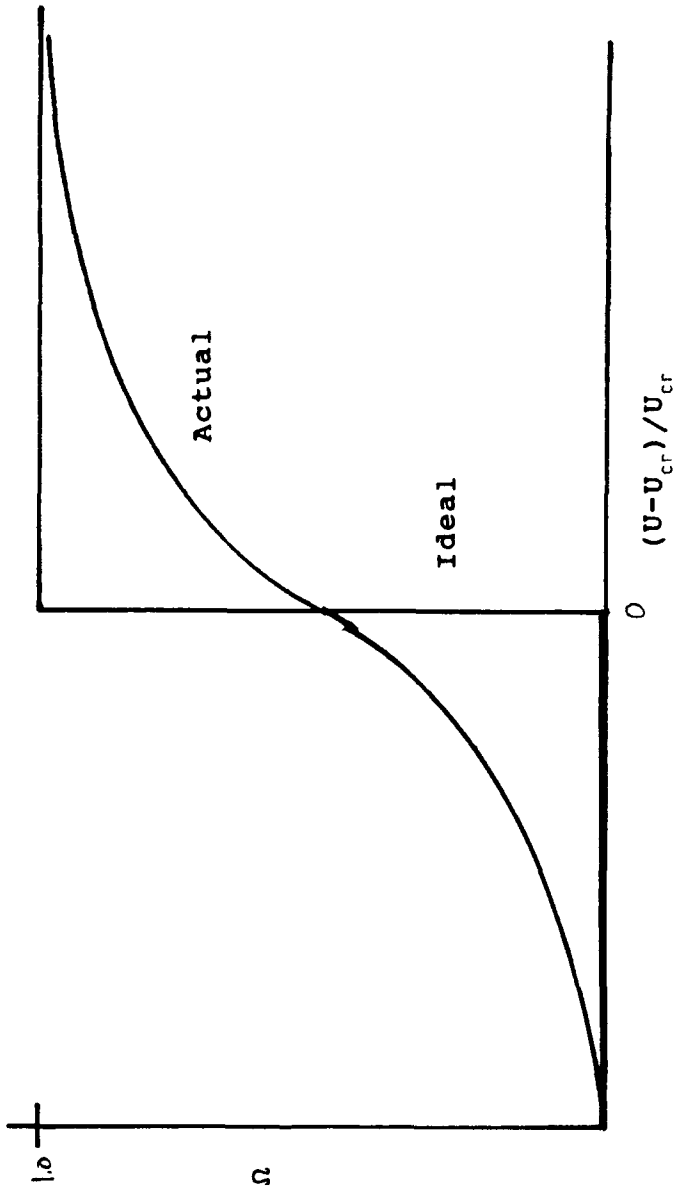

Figure 5.6 Pickup Parameter vs. Dimensionless Critical Velocity

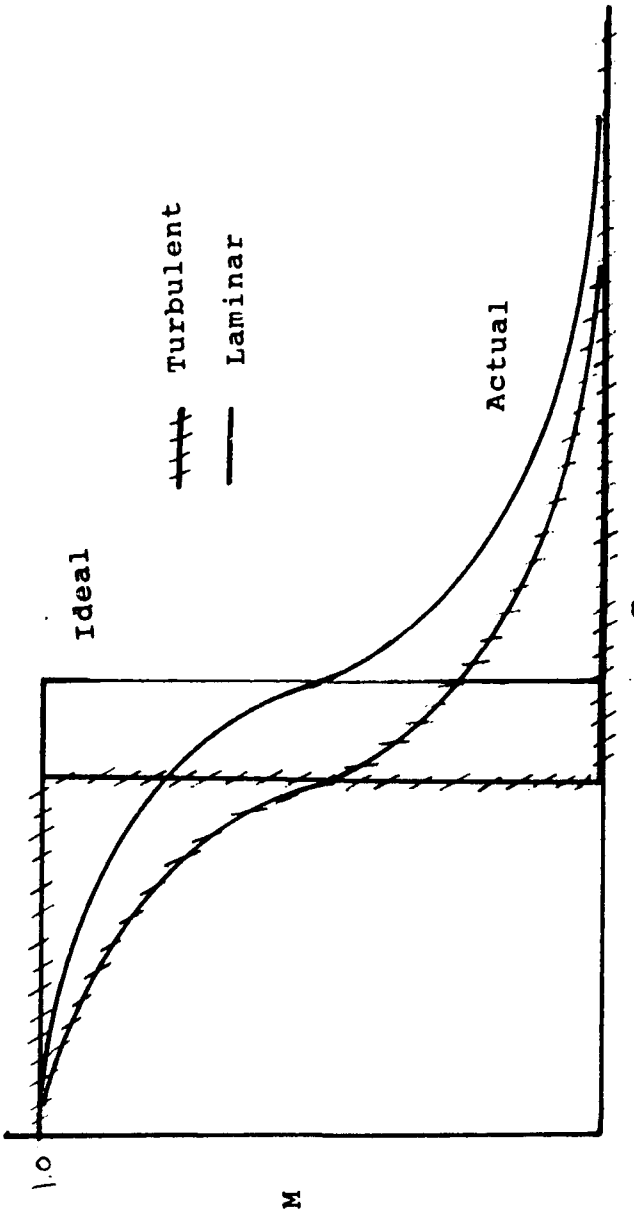

Figure 5.7 Deposition Parameter vs. Dimensionless Critical Velocity

critical value. The deposition curves are negatively skewed because the critical velocity required for pickup is greater than that required for deposition.

Combining Figure 5.6 and 5.7 provides a view of the efficiency parameter since $\xi'=(\Omega-M)$. Figure 5.8 provides the shape and characteristics of the efficiency parameter curve. Since no upstream sediment concentration is considered, ξ' ranges from zero to one. The ξ' must be calibrated and verified by field and laboratory data before it can be used practically.

Since the data is not presently available to determine ξ', it is assumed that ξ' is a meaningful parameter and could be determined as a function of the variables affecting the pickup and deposition parameters. It is important to note that as the flow becomes saturated with sediment, ξ' approaches zero. Once the flow can no longer support additional sediment transport, ξ' is zero within that saturated reach. A graphical representation is given in Figure 5.9.

The procedure developed in this thesis is to be applied assuming the sediment transport efficiency parameter is known or can be computed. The actual method used to obtain ξ is left to others to develop in future research from either experimentation or theory. The theoretical procedure would be to obtain ξ directly from the Ω - M relationship since both all are a function of the same variables. In a

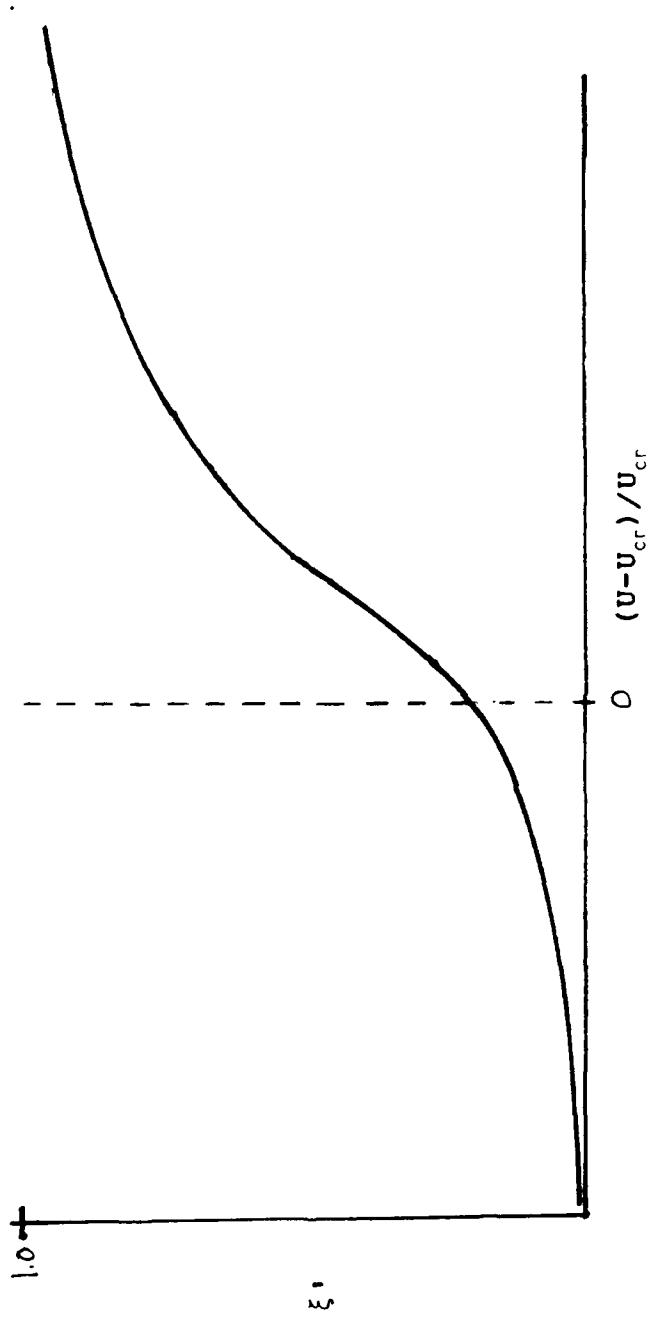

Figure 5.8 Efficiency vs. Dimensionless Critical Velocity

Figure 5.9 Variation of ξ' with Sediment Concentration

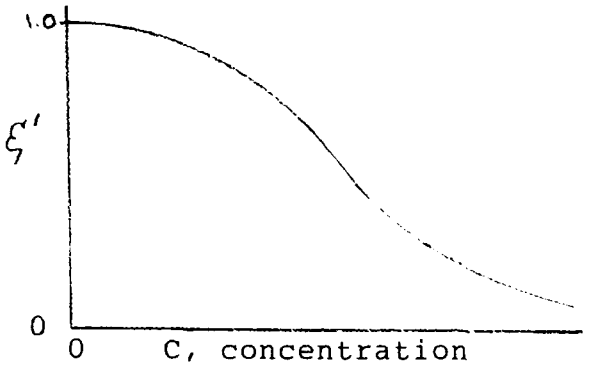

laboratory setting, ξ can be obtained by using flume data where ξ is obtained as a function of time or space depending upon the arrangement of the flume and the data recorded. Once the ξ relationship is developed, the transport efficiency parameter can be applied to different situations and conditions.

For ease of use, a dimensionless efficiency parameter is given by

$$\xi = \frac{(\Omega - M)}{\Omega} \qquad (5.25)$$

5.3 SEDIMENT TRANSPORT EQUATION

The transport rate can be approximated by using an assumed transport efficiency, ξ, and given a procedure to

determine whether the flow is sufficient to induce particle motion. The sediment transport term, q_s, is defined as the total sediment volume transported per unit width of the channel and per unit time. From the continuity equation shown previously, the general form of the equation is

$$q_s = q_{s1} + \frac{dq_s}{dx}\Delta x = q_{s1} + n\xi V_s \Delta x \qquad (5.25)$$

where n = number of particles per unit bed area,

ξ = the transport efficiency parameter,

V_s = volume of a sediment particle,

Δx = length of the channel segment.

A plot of $T_s/q\ t_d$ vs. time/t_d is given as Figure 5.10. Since the Eq. 5.23 represents the sediment transport rate for a unit time, the total transport for an entire event of duration t_d, T_s, over a length x=0 to x=L_0 with q_{s0}= 0, is

$$T_s = \int_0^{t_d} \left(\int_0^{L_0} \xi'(x,t)\ n(x,t)\ V_s dx \right) dt \qquad (5.29)$$

For $L_0 = \Sigma\ \Delta x$ and duration $t_d = \Sigma\ \Delta t$ with ξ' invariant with time but variable with space,

$$T_s = \sum_{i=1}^{t_d} \sum_{j=1}^{L_0} \left[(\xi_j (1-\xi_j)^{i-1} n_j V_s \Delta x) \right] \qquad (5.29)$$

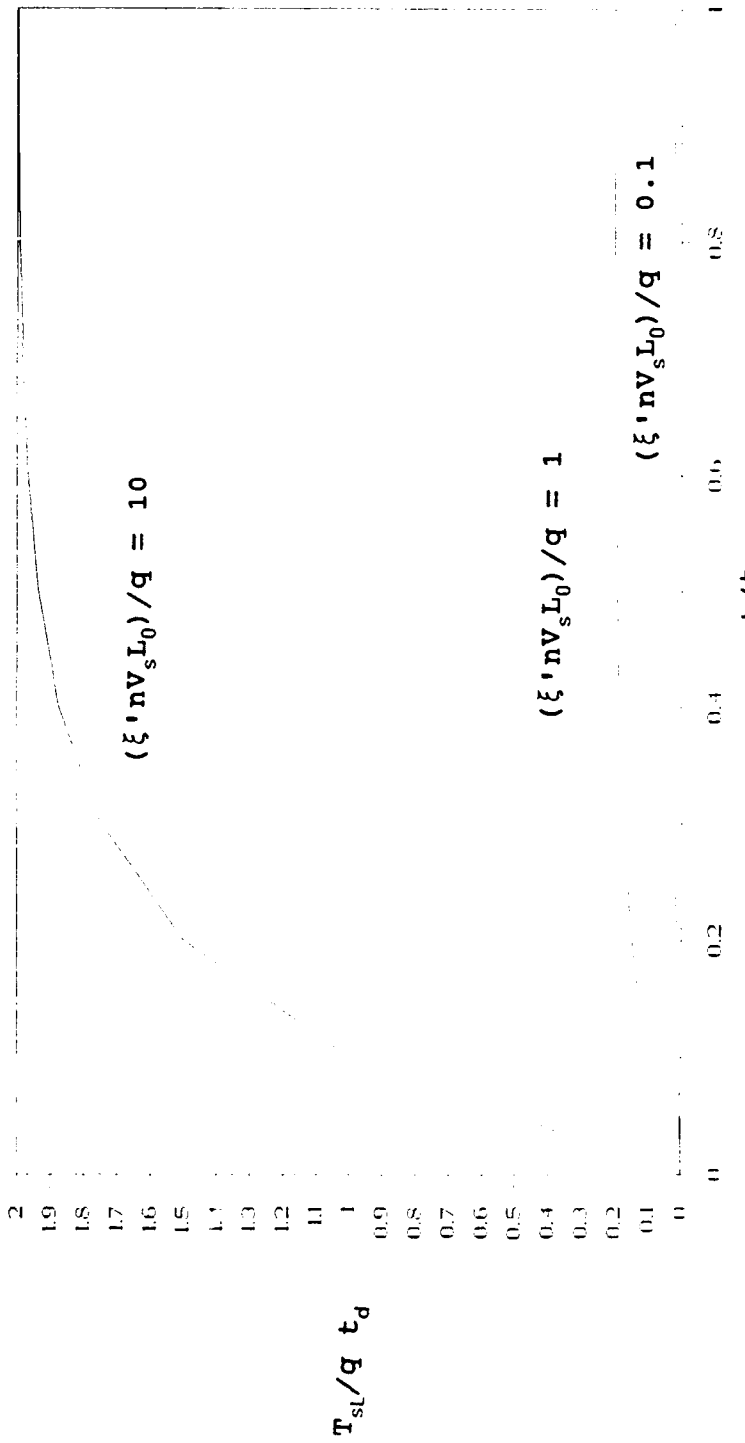

Figure 5.10 Total Sediment Transport vs. Time

since for any given Δx the amount of sediment on the bed at the ith Δt is $(1-\xi')nV_s$ and the sediment transport is $\xi'(1-\xi')^{i-1}nV_s$. Figure 5.11 provides a plot of T_{slt}/T_{sltd} vs. time/t_d where T_{slt} is the total sediment transport per unit time and T_{sltd} is the total sediment transport per the entire event. Eq. 5.25 expresses the total sediment transport, T_s, as a volume per unit width. Although mass is easier to measure and more commonly used, volume provides a suitable variable from the physical viewpoint. Also, mass can be easily found by knowing V_s and ρ_s or γ_s. As mentioned previously in Section 5.2 and Figure 5.8, ξ' decreases as the sediment concentration increases. Therefore, Eq. 5.25 (finite one) is valid only for low concentrations where ξ' is approximately constant. Figure 5.12 shows a graph of the dimensionless parameters q_s/q versus x/h computed using

$$\frac{q_{sx}}{q} = \frac{\xi' n V_s}{U} \frac{x}{h} \tag{5.30}$$

However, the transport efficiency parameter is most likely not constant throughout the channel reach. As the flow becomes saturated with sediment and is no longer able to induce additional transport, the efficiency should decrease to zero. The decrease of ξ must be determined by data analysis. However, an assumed relationship is used in this study. Figure 5.13 graphs q_s/q versus x/L_0 for a decaying ξ'. The decay relationship is assumed to be an

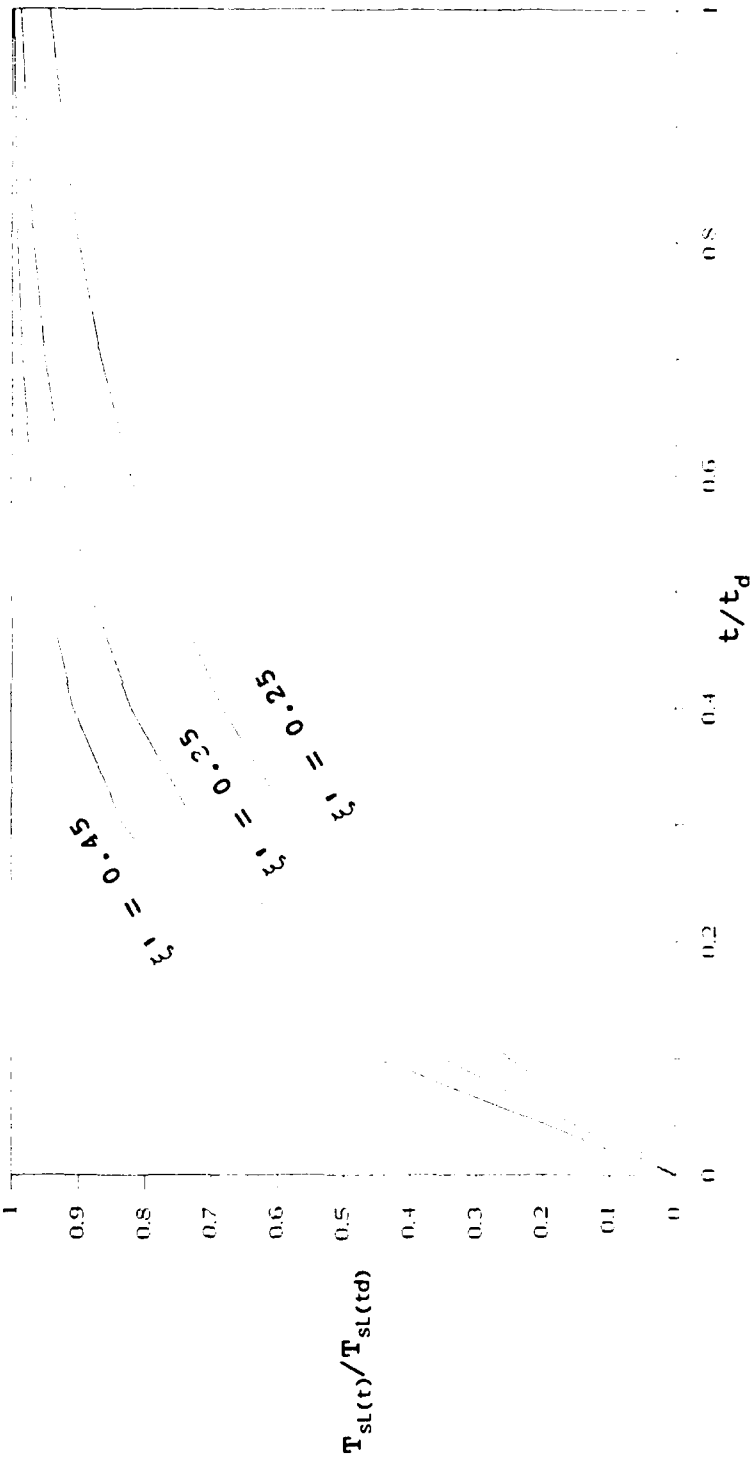

Figure 5.11 Total Sediment Transport vs. Time

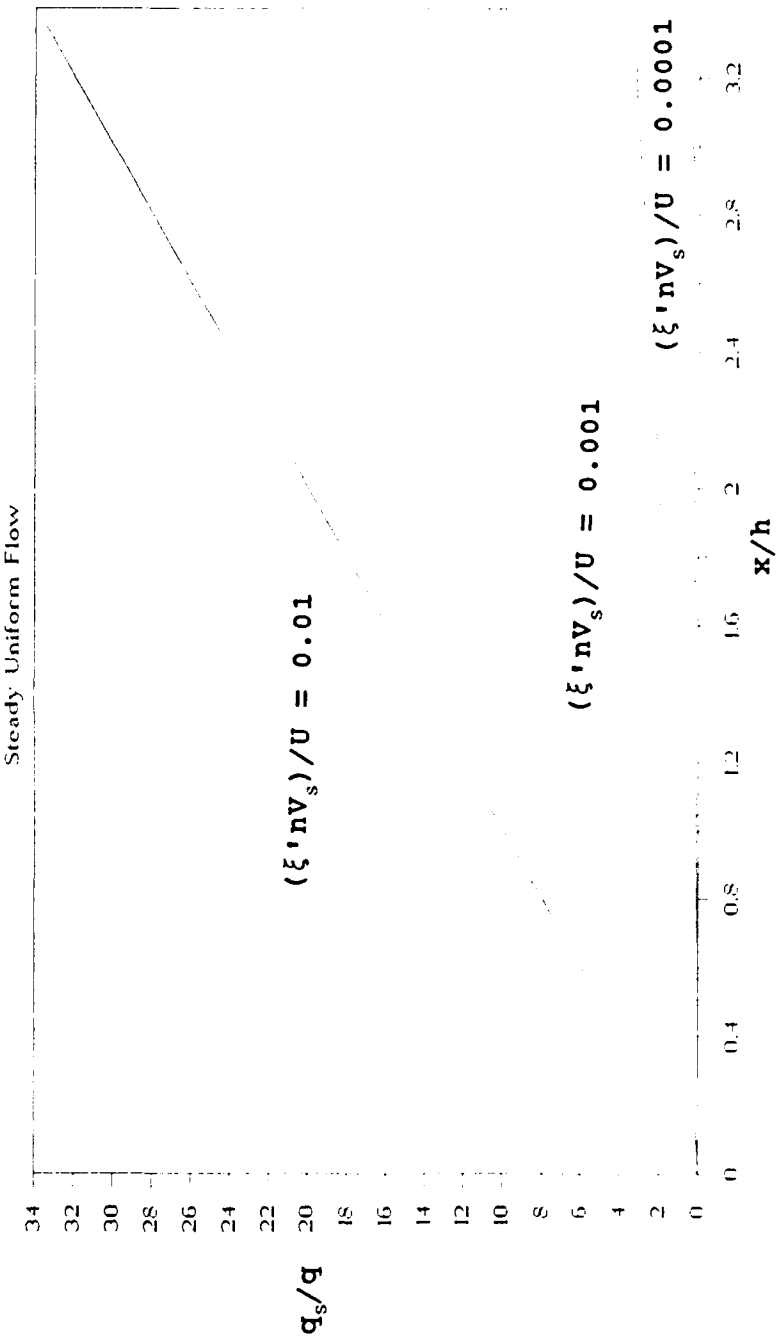

Figure 5.12 Plot of q_s/q vs. x/h

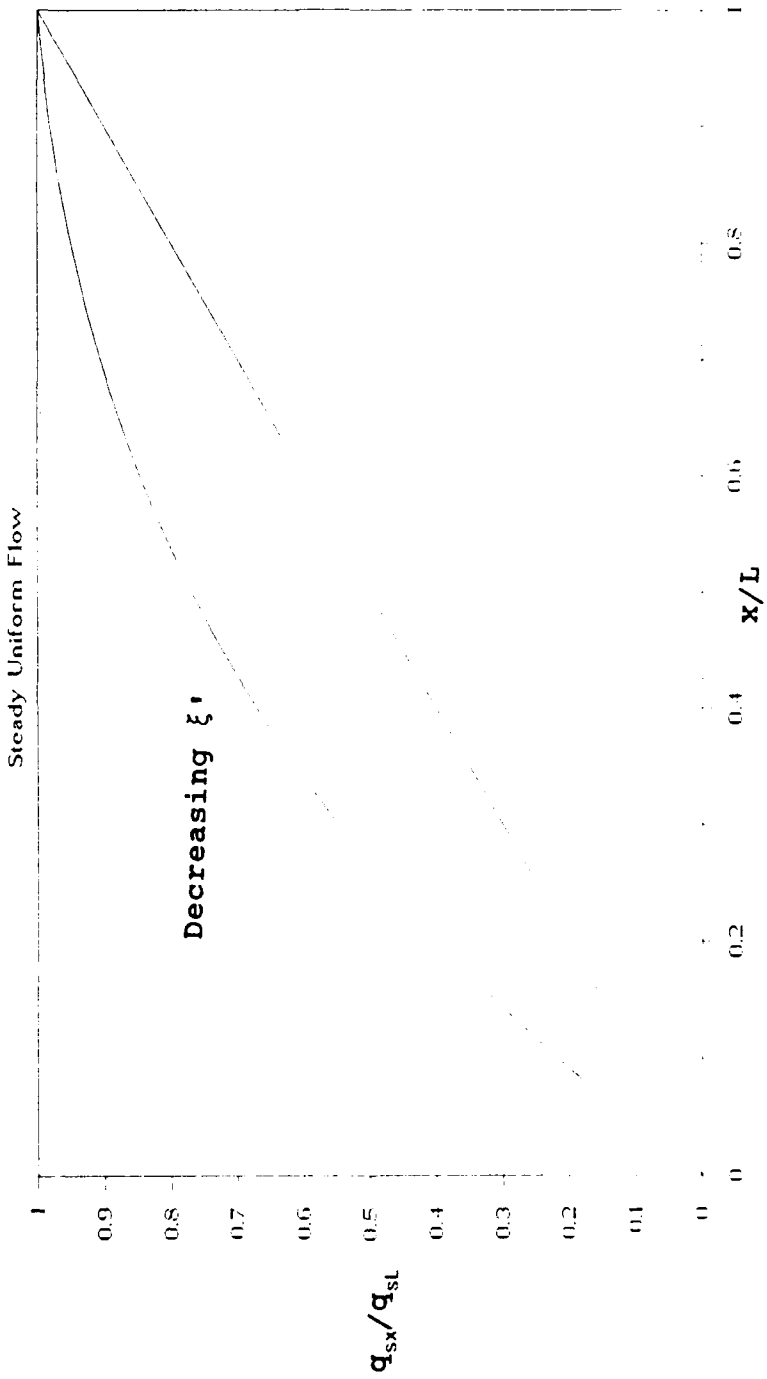

Figure 5.13 Plot of q_s/q vs. x/L_0 with Decreasing ξ

exponential one of the form

$$\xi = \xi_0 \, e^{-kx} \qquad (5.31)$$

where k is the decay rate (1/length).

Figure 5.14 $q_s/q_{s\ max}$ versus Sediment Concentration

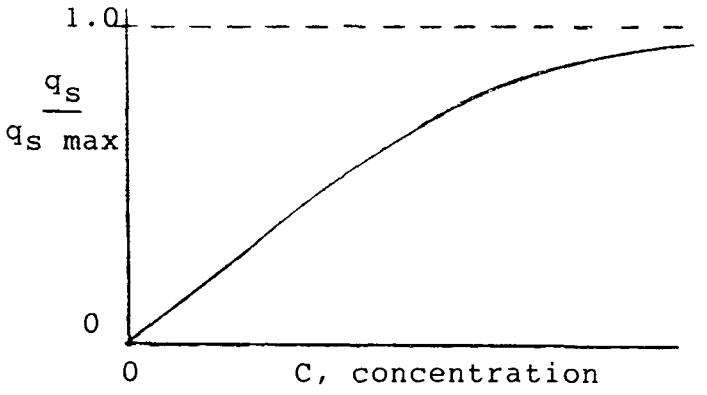

The sediment transport capacity of the flow may never approach saturation if: the efficiency is constant; the sediment concentration is very sparse; or the channel length is comparatively short. See Figure 5.14. Under one or more of the above conditions, the plot of q_s/q under consideration will be a straight line instead of the presumed line asymptotic to the saturation level. Such may be the case on an airfield pavement where the channel is relatively short (i.e. across the runway or apron). Therefore, the estimation of a constant ξ may be valid for this particular case.

6. RESULTS & DISCUSSION

6.1 RESULTS

Since field or laboratory data is not available for sediment transport in shallow flow, hypothetical data is used to test the model developed in the previous section. Figure 5.12 shows a plot of q_s/q versus x/h. The shape of the curve and the magnitude of the values seem reasonable given the physical view of the process and the selected values of the variables.

Although a lack of available data prevents a calibrated and verified quantitative model, a qualitative one is provided by the research in this thesis. This model can be applied to simulate sediment transport in shallow steady uniform flow over an impervious surface. Future expansion of the results presented here will allow the model to be used for nonuniform and unsteady flows also. Therefore, the objective of the thesis has been obtained in the form of a model which predicts the total sediment transport in a shallow flow over an impervious surface.

6.2 DISCUSSION

6.2.1 Sediment Transport Parameters

The major parameters presented in this study are the incipient motion parameter, $U_{cr}/\sqrt{gd_s}$, and the transport efficiency parameter, ξ'. The use of dimensional analysis and the approach from general physics helps to verify the validity of these two parameters. The employment of the Boussinesq type coefficients ensure the incipient motion parameter accounts for the particular velocity distribution (laminar or turbulent) and the small flow depth to sediment size ratio. Unfortunately, a value for the transport efficiency parameter cannot be obtained due to the lack of data. However, this parameter is valid and the model can account for variation of ξ. An expression for ξ as a function of the other sediment transport variables was not developed due to the complex nature of the flow and the lack of data. Although the efficiency is assumed constant over the entire length of the channel under consideration, a constant ξ may be applicable to the actual case of sediment transport in shallow flow over an impervious surface such as an airfield.

6.2.2 Impact of Variables Not Considered

Due to the complexity of the problem of particle movement in a moving fluid, many variables have not been considered as a separate parameter in this study. Unsteady flow, the impact of rainfall, and the effect of mutual interference of multiple particles are three such additional parameters. The impact and approach to inclusion of each parameter is discussed below.

Unsteady flow can be included in the sediment transport parameter by modeling the velocity distribution. The same general form of the equations presented earlier are still valid. However, the coefficients, such as β, will be different. Also, in order to account for unsteady flow, the model would require a great deal more data. One example is the variation of the velocity with time which would be required to replace the average velocity. This requirement for additional data would most likely not be greater than the benefit of a more accurate model.

The effect of rainfall on sediment transport on erodible boundaries has been studied in recent years. Generally, it is presented that the impact of the raindrops imparts energy to the control volume. The friction slope term, S_f, is often modified to include the effects of the raindrop impact. However, no work has been found which studied rainfall impact on sediment transport over an

impervious, nonerodible boundary. Much laboratory flume work is required to establish the necessary relationships of the raindrop variables with the sediment transport variables presented here earlier.

Only a single particle was considered in the earlier theory section. Figure 6.1 depicts the forces acting on submerged, adjacent particles. In order to relate these forces, a new term is introduced. The term F_p denotes the "pushing" force given to one particle by another. As seen in the figure, the major impedance to the movement of particle number 2 is the shielding it receives from particle 1. This shielding prevents particle 2 from receiving the full impact of the flow. As stated before, the term A_{sn}, particle surface area normal to flow, can partially account for the shielding. However, this term does not account for the variation of flow caused by particle 1, i.e. the flow separation and resulting low pressure area which will develop immediately behind particle 1. This pressure reduction results in greater drag on particle 1 but will tend to decrease the total drag on particle 2.

This decrease in total drag on particle 2 is due to the decreased (actually, negative according to the defined coordinates) pressure drag on the particle. The pressure drag and skin friction combine to account for the total drag. The term C_D, drag coefficient, accounts for both types. This effect of reduced drag on the shielded particle

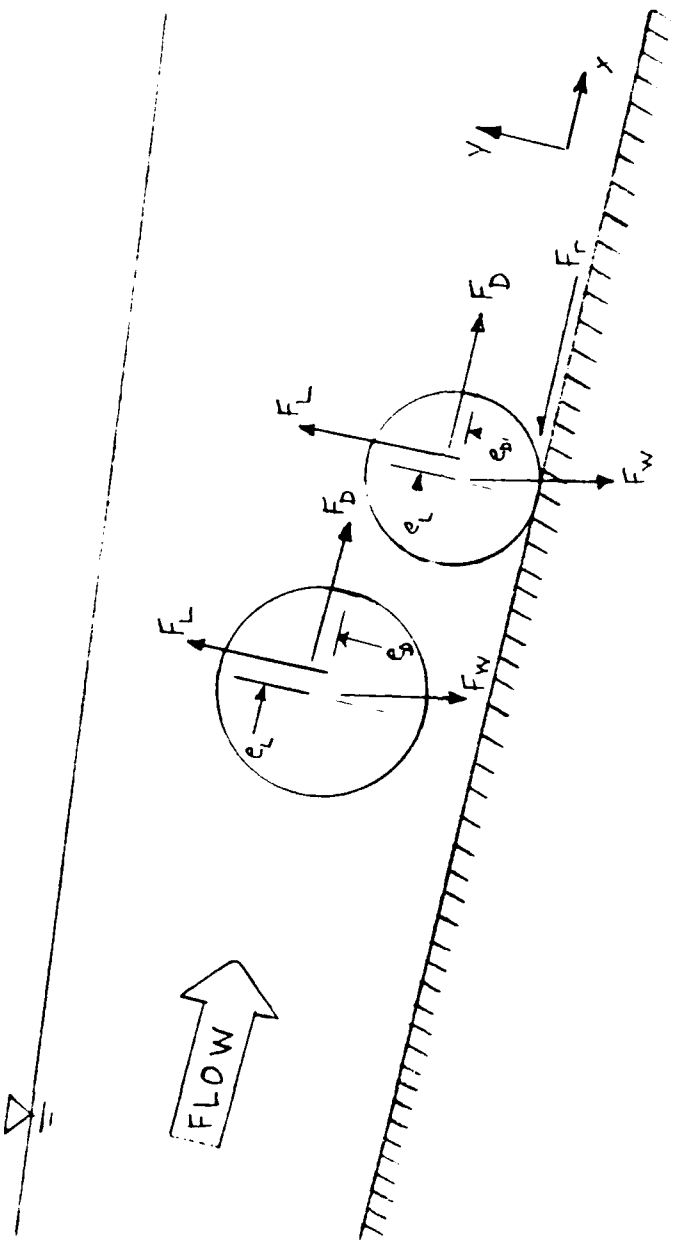

Figure 6.1 Forces on Submerged, Adjacent Particles

will vary greatly according to the flow regime, laminar to fully developed turbulent. At low Reynolds number, Re < 0.1 - 1.0, the flow is considered creeping and skin friction drag is predominate (Shames, 1982). Therefore, the effect is minimal. However, as Re increases, Re $\approx 5x10^3$, separation occurs and pressure drag becomes important (Shames, 1982). When the flow becomes increasingly turbulent, the pressure drag is reduced because the turbulent flow is better able to adhere to the curved surface of the particle and resist separation.

When the pressure behind particle 1 is reduced, particle 2 will tend to move toward particle 1. This is due to the larger pressure behind particle 2 (supposing no other particles are close to particle 2). However, the movement of the two particles toward each other will increase the fluid pressure between the two particles. When this increased pressure becomes greater than the pressure behind particle 2, the particles will begin to move away from one another. This action of particle movement toward and away from each other can be accounted for by the "pushing" force term, F_p. However, details one the magnitude or makeup of this term are not yet known.

A conspicuous assumption used in the model presented here is that the sediment transport rate can be found by relating it to conditions of incipient motion rather than modeling the sustained movement of the particle. However,

this approach is the one generally taken by those studying sediment transport in alluvial cases. The complexities and lack of greater physical understanding of the equation of motion for the particles virtually require such an approach.

6.2.3 Application of the Model

The sediment transport procedure developed in this thesis can be applied given values for the required data. Sediment variables include d_s, ρ_s, nV_s, and ξ. The first two are found from analysis of the field data sample. The term nV_s can be used to replace A^p, the areal sediment packing, and expresses the total volume of sediment available for transport. Since the particle diameter is known, the particle volume is easily calculated for the case of a sphere. The volume of a non-spherical particle could be related to that of a spherical one by the use of the shape factor, SF. Since the total volume is sought, the actual number of particles, n, is not required. This total volume variable, nV_s, could be obtained by statistical methods which relate the total available volume to factors such as location, rain-free days, frequency of street cleaning, etc. for urban environments. It must be noted however, that the airport environment greatly differs from that of the urban one, mainly because the jet engine blast from the aircraft will continuously move the sediment. The actual method

employed to determine the available source of sediment is a problem not addressed in this work.

Fluid variables include ρ, q, h, μ, γ, and β. For rainfall, ρ, μ, and γ are fairly constant and known. The flow rate q, and flow depth h can be measured directly in the field. Given the geometry of the flow, either q or h could be replaced by U, the mean flow velocity since $q = hU$. β is provided in Section 4.3. Flow variables are S_0 and L_0 which can be found directly from the field.

Therefore, the only variable above which is not easily found or expected to be found with reasonable means is ξ, the sediment transport efficiency parameter. The procedure to determine this variable is left to others as outlined in Section 5.3.

Particles of different sizes or densities can be accounted for in the model by classifying the different sizes or densities into groups, computing the transport for each group and then adding the transport values together for a total. This assumes a linear approximation is appropriate. Further study is required to verify this assumption.

7. CONCLUSIONS AND RECOMMENDATIONS

A physically based procedure to simulate sediment transport is presented for the case of shallow flow over an impervious surface. The procedure is developed for particulate matter only and would not apply to oils, fibrous material, or dissolved pollutants. This model accounts for either a laminar flow following a parabolic distribution or turbulent flow over a smooth or rough boundary following a logarithmic distribution or a power distribution. Momentum flux correction factors and established are presented to account for the variable velocity distribution and varying flow depth to particle size ratio.

No field or laboratory flume data was collected as part of this research. Such data was not found available in past research by others although this particular case of sediment transport seems to be gaining interest in the academic environment. Although the model is not verified by actual data, hypothetical data is used to show the relationships developed herein. All graphs contained the shapes and characteristics expected from physical knowledge.

Because of this lack of calibration and verification, the model should not be applied to any actual case for prediction purposes until tested. As Bagnold (1966) stated:

> "Indeed the outlook is obscured by the very number of published theories. For example, the engineer

> research student, encouraged by degree thesis requirements to advance a new theory rather than to verify existing concepts, is able to find somewhere in the literature, and to quote, support for an assumption which best suites his argument."

Usually, a sensitivity analysis is conducted to reflect the sensitivity of the model to each parameter. Therefore, the parameters, when erroneous, are identified which impart the most error in the model. No sensitivity analysis was accomplished in this thesis since the data is not available to fully test the model. Since the data must have sufficient accuracy in order to have a meaningful uncertainty range, a sensitivity analysis would not be helpful in this work. However, the graphs presented in Section 5.3 are given as functions of dimensionless parameters in order to reduce any sensitivity of the model to a particular variable.

The major recommendation for future study is the collection of applicable laboratory flume and field data. This data is necessary to verify the relationships established in this study and provide means to expand and detail these relationships. Section 6.2.2 discusses several variables which were not fully incorporated into the procedure developed in this thesis. The expansion of the model to fully incorporate these variables is a requirement

of future study. These variables include: rainfall; particles of varying shapes, sizes, and densities; and nonuniform and unsteady flow. Future study is required to develop the sediment transport efficiency parameter. Also, a method to determine the total available sediment is needed.

REFERENCES

Ackers, P. and W. R. White. 1973. Sediment Transport: New Approach and Analysis. Jour. Hyd. Div. Proc. ASCE, 99(HY11):2041-2060.

Albertson, M. L. 1953. Effect of Shape on the Fall velocity of Gravel Particles. Proceedings of the Fifth Hydraulics Conference, State University of Iowa, Studies in Engineering Bulletin 34. pp243-261.

Ananian, A. K. and E. T. Gerbashian. 1965. About the System of Equations of the Movement of Flow Carrying Suspended Matter. Journal of Hydraulic Research, 3:20-30.

Bagnold, R. A. 1966. An approach to the sediment transport problem from general physics. U.S. Geological Survey Professional Paper 422J.

Brownlie, W. R. 1985. Compilation of Alluvial Channel Data. Jour. Hyd. Eng. ASCE, 111(7):1115-1119.

Chadwick, A. J. and J. C. Morfett. 1986. Sediment Transport. Chapter 9. In: Hydraulics in Civil Engineering. Allen and Unwin, London, England.

Chen, C. L. 1976. Flow Resistance in Broad Shallow Channels. Jour. Hyd. Div. Proc. ASCE, 102(HY3):307-322.

Chow, V. T. 1964. Handbook of Applied Hydrology. McGraw-Hill Book Co., New York, NY.

Chow, V. T. 1959. Open Channel Hydraulics. McGraw-Hill Book Co., New York, NY.

Cooper, R. H. 1970. A Study of Bed-Material Transport Based on the Analysis of Flume Experiments. Ph.D. Thesis. University of Alberta. Edmonton, Alberta, Canada.

Cooper, R. H., A. W. Peterson, and T. Blench. 1972. Critical Review of Sediment Transport Experiments. Jour. Hyd. Div. Proc. ASCE, 98(HY5):827-843.

Engman, E. T. 1986. Roughness Coefficients for Routing Surface Runoff. Jour. Ir. and Drain. Eng. Div. ASCE, 112(1):39-53.

Glass, L. J. and E. T. Smerdon. 1967. Effect of rainfall on the velocity profile in shallow-channel flow. Trans. ASAE, 10(3):330-332,336.

Graf, W. H. 1984. Hydraulics of Sediment Transport. Water Resources Publications, Littleton, CO. 513 p.

Guy, Brian T. 1990. Investigation of Sediment Transport at the Capacity Rate in Interrill Flow. M.S. Thesis. University of Guelph, Ontario, Canada.

Hino, M. 1963. Turbulent Flow with Suspended Particles. Jour. Hyd. Div. Proc. ASCE, 89(HY4):161-185.

Hobbs, P. V. and T. Osheroff. 1967. Splashing of Drops on Shallow Liquids. Science, 158(9):1184-1186.

Izzard, C. F. 1944. The surface-profile of overland flow. Trans. AGU, 25:959-968.

Julian, P. Y. and D. B. Simons. 1985. Sediment Transport Capacity of Overland Flow. Trans. ASAE, 28(3):755-762.

Kuhlemeyer, R. L. and D. B. Warner. 1963. Discussion of "Spatially Varied Flow from Controlled Rainfall", by D. C. Woo and E. F. Brater. Jour. Hyd. Div. Proc. ASCE, 89(HY4):233-240.

Laws, J. O. 1941. Measurement of the fall velocity of waterdrops and rain drops. Trans. AGU, 22:709-721.

Li, Wen-Hsiung. 1955. Open Channels with Nonuniform Discharge. Trans. ASCE, 120:255-280.

MacDougal, C. H. 1933. Bed sediment transportation in open channels. Trans. AGU, 14:pp 491-495 (June).

Macklin, W. C. and G. J. Metaxas. 1976. Splashing of Drops on Liquid Layers. Jour. Appl. Physics, 47(9):3963-3970.

Macklin, W. C. and P. V. Hobbs. 1969. Subsurface Phenomena and the Splashing of Drops on Shallow Liquids. Science, 166(10):107-108.

Marshall, J. S. and W. Palmer. 1948. The Distribution of Raindrops with Size. Jour. Meteorology, 5:165-166.

Mutchler, C. K. and C. L. Larson. 1971. Splash Amounts from Waterdrop Impact on a Smooth Surface. Water Resources Research, 7(1):195-200.

Podmore T. H. and L. F. Huggins. 1980. Surface Roughness Effects on Overland Flow. Trans. ASAE, 23(6):1434-1439, 1445.

Robeson, J. A. and C. T. Crowe. 1985. Engineering Fluid

Mechanics. Houghton Mifflin Company, Boston, MA.

Rottner, J. 1959. A formula for bed-load transportation. La Houille Blanche, 14:285-307.

Rouse, H. (editor). 1959. In: Advanced Mechanics of Fluids. John Wiley and Sons Inc., New York, NY.

Rouse, H. 1965. Critical Analysis of Open-Channel Resistance. Jour. Hyd. Div. Proc. ASCE, 91(HY4):1-25.

Rouse, H., H. J. Koloseus, and J. Davidian. 1963. The Role of the Froude Number in Open-Channel Resistance. Journal of Hydraulic Research, 1:14-19.

Rouse, H. and J. S. McNown. 1945. Discussion of "Coefficients for Velocity Distribution in Open-Channel Flow." by W. S. Eisenlohr, Jr. Transactions ASCE, 110:651-657.

Sadeghian, M. R. 1990. Overland Flow on Disturbed Soil. Ph.D. Thesis. Univ. of Illinois at Urbana-Champaign, Urbana, IL.

Schlichting, H. 1968. Turbulent Boundary Layers. Part. D. In: Boundary-Layer Theory. 7th Ed. McGraw-Hill Book Co., New York, NY.

Schroeter, H. O. and W. E. Watt. 1989. Practical Simulation of Sediment Transport in Urban Runoff. Canadian Journal of Civil Engineering, 16:704-711.

Shames, I. H. 1982. Mechanics of Fluids. McGraw-Hill Book Co. New York, NY. 692 p.

Shen, H. W. and Ruh-Ming Li. 1973. Rainfall Effect on Sheet Flow over Smooth Surface. Jour. Hyd. Div. Proc. ASCE, 99(HY5):771-792.

Simons, D. B. and F. Şentürk. 1976. Sediment Transport Technology. Water Resources Publications, Fort Collins, CO. 807 p.

Stein, R. A. 1965. Laboratory studies of total load and apparent bed load. Journal of Geophysical Research, 70(8), April 1965.

Strelkoff, T. 1969. One-Dimensional Equations of Open-Channel Flow. Jour. Hyd. Div. Proc. ASCE, 95(HY3):861-876.

Tan, S. 1989. Rainfall and Soil Detachment. Journal of Hydraulic Research, 27(5):699-715.

Vanoni, V. A. 1946. Transportation of Suspended Sediment by Water. Trans. ASCE, 111:67-133.

Vanoni, V. A. (editor). 1977. Sedimentation Engineering. ASCE, New York, NY. 745 p.

Vanoni, V. A. 1984. Fifty Years of Sedimentation. Journal of Hydraulic Engineering. ASCE, 110(8):1022-1057.

Wenzel, H. G. 1970. The Effects of Raindrops Impact and Surface Roughness on Sheet Flows. Water Resources Research Report No. 34, Univ. of Illinois, Urbana, IL.

Woo, D. and E. F. Brater. 1962. Spatially Varied Flow from Controlled Rainfall. Jour. Hyd. Div. Proc. ASCE, 88(HY6):31-56.

Yalin, M. S. 1977. Mechanics of Sediment Transport. Pergamon Press, Oxford, England. 298 p.

Yalin, M. S. 1971. Similarity in Sediment Transport. Chapter 6. In: Theory of Hydraulic Models. Macmillan, London, England.

Yang, C. T. 1973. Incipient Motion and Sediment Transport. Jour. Hyd. Div. Proc. ASCE, 99(HY10)::1679-1704.

Yen, B. C. 1973. Open-Channel Flow Equations Revisited. Jour. Eng. Mech. Div. Proc. ASCE, 99(EM5):979-1009.

Yen, B. C. 1986. Rainfall-runoff Process on Urban Catchments and Its Modeling. In: Urban Drainage Modeling, Proceedings of the International Symposium on Comparison of Urban Drainage Models with Real Catchment Data, Dubrovnik, Yugoslavia. Pergamon Press, Oxford, UK. 3-26.

Yen, B. C. and H. G. Wenzel. 1970. Dynamic Equations for Steady Spatially Varied Flow. Jour. Hyd. Div. Proc. ASCE, 96(HY3):801-814.

Yen, B. C., H. G. Wenzel, and Y. N. Yoon. 1972. Resistance Coefficients for Steady Spatially Varied Flow. Jour. Hyd. Div. Proc. ASCE, 98(HY8):1395-1410.

Yoon, Y. N. and H. G. Wenzel, Jr. 1971. Mechanics of Sheet Flow Under Simulated Rainfall. Jour. Hyd. Div. Proc. ASCE, 97(HY9):1367-1386.

Yu, Y. S. and J. S. McNown. 1964. Runoff from impervious surfaces. Journal of Hydraulic Research, 2(1):3-24.